Phenotypic and transcriptomic analyses reveal major differences between apple and pear scab nonhost resistance

Emilie Vergne, Chevreau E., Ravon E., Gaillard S., Pelletier S., Bahut M., Perchepied L.

Title

Phenotypic and transcriptomic analyses reveal major differences between apple and pear scab nonhost resistance

Authors

Vergne E.[1*], Chevreau E.[1*], Ravon E.[1], Gaillard S.[1], Pelletier S.[1], Bahut M.[2], Perchepied L.[1]

Affiliations

[1] Univ Angers, Institut Agro, INRAE, IRHS, SFR QUASAV, F-49000 Angers, France

[2] Univ Angers, SFR QUASAV, F-49000 Angers, France

*E. Vergne and E. Chevreau made equal contributions to this work.

Corresponding author

E.Vergne

Emilie.vergne@inrae.fr

Abstract

Background. Nonhost resistance is the outcome of most plant/pathogen interactions, but it has rarely been described in Rosaceous fruit species. Apple (*Malus x domestica* Borkh.) is a nonhost for *Venturia pyrina*, the scab species attacking European pear (*Pyrus communis* L.). Reciprocally, *P. communis* is a nonhost for *Venturia inaequalis*, the scab species attacking apple. The major objective of our study was to compare the scab nonhost resistance in apple and in European pear, at the phenotypic and transcriptomic levels.

Results. Macro- and microscopic observations after reciprocal scab inoculations indicated that, after a similar germination step, nonhost apple/*V. pyrina* interaction remained nearly symptomless,

whereas hypersensitive reactions were observed during nonhost pear/*V. inaequalis* interaction. Comparative transcriptomic analyses of apple and pear nonhost interactions with *V. pyrina* and *V. inaequalis*, respectively, revealed considerable differences. Very few differentially expressed genes were detected during apple/*V. pyrina* interaction, which is consistent with a symptomless type I nonhost resistance. On the contrary, numerous genes were differentially expressed during pear/*V. inaequalis* interaction, as expected in a type II nonhost resistance involving visible hypersensitive reaction. Pre-invasive defense, such as stomatal closure, was detected, as well as several post-invasive defense mechanisms (apoplastic reactive oxygen species accumulation, phytoalexin production and alterations of the epidermis composition). In addition, a comparative analysis between pear scab host and nonhost interactions indicated that, although specificities were observed, two major defense lines were shared in these resistances: cell wall and cuticle modifications and phenylpropanoid pathway induction.

Conclusion. This first deciphering of the molecular mechanisms underlying a nonhost scab resistance in pear offers new possibilities for the genetic engineering of sustainable scab resistance in this species.

Keywords: apple, pear, nonhost resistance, transcriptomics

Background

Apple (*Malus domestica* Borkh.) and European pear (*Pyrus communis* L.) are two closely related species belonging to the *Rosaceae* family. Reclassification of the *Rosaceae* placed both *Pyrus* and *Malus* genera in the subfamily *Spiraeoideae*, tribe *Pyreae* and subtribe *Pyrinae,* this subtribe corresponding to the long-recognized subfamily *Maloideae* [1]. Efforts to resolve relationships within this subtribe have frequently failed, and Campbell et al [2] concluded that the genera of this subtribe *Pyreae* have not diverged greatly genetically. The recent sequencing of the pear genome [3] allowed a precise comparison with the apple genome [4] and led to the estimation of a divergence time

between the two genera of ≈ 5.4 – 21.5 million years ago. Furthermore, apple and pear genomes share similar chromosome number (n=17), structure and organization.

Scab disease, caused by *Venturia* spp., affects several rosaceous fruit tree species. These hemibiotrophic pathogens can infect only a limited host-range during their parasitic stage, but they can overwinter as saprophytes in the leaf litter of a larger range of plant species [5]. Scab disease is caused by *V. inaequalis* on apple, by *V. pyrina* (formerly named *V. pirina* [6]) on European pear, and by *V. nashicola* on Japanese (*P. pyrifolia* Nakai) and Chinese (*P. ussuriensis* Maxim) pears. Cross inoculations of *Venturia* spp. on different rosaceous fruit trees indicates that these pathogens are highly host specific, probably indicating a close co-evolution of these pathogens with their hosts [7].

A plant species unable to be successfully infected by all isolates of a pathogen species is considered as a nonhost for this pathogen. Nonhost interactions of *Venturia* spp. on apple and pear have rarely been described. Microscopic observations have been made on *P. communis / V. nashicola* [8] as well as *M. domestica* / *V. pirina* and *P. communis* / *V. inaequalis* [5, 9]. In all cases, conidia germinated and produced appressoria and runner hypheae, but failed to establish a network of stroma. No macroscopic symptoms were visible.

Because of its durability, nonhost resistance has attracted numerous studies over the last decade, which have uncovered its multiple and complex defense components. The underlying mechanisms of nonhost resistance comprise pre-invasion resistance with preformed or induced cell-wall defenses, metabolic defense with phytoanticipin or phytoalexin accumulation, pattern-triggered immunity (PTI) as well as elicitor-triggered immunity (ETI) and various signaling pathways [10]. To our knowledge, the molecular bases of scab nonhost resistance of apple and pear have never been investigated. The objectives of our study were 1) to precisely describe nonhost resistance symptoms in *M. domestica* / *V.pyrina* and *P. communis* / V. *inaequalis* interactions 2) to analyze the underlying molecular mechanisms of both nonhost interactions through a transcriptomic study 3) to compare the mechanism of host [12] and nonhost scab resistance in apple and European pear.

Results and discussion

Variable symptoms of nonhost resistance

Nonhost interactions were observed in a test performed on 'Gala' and 'Conference', all inoculated by a *V. pyrina* strain (VP102) and a *V. inaequalis strain* (VI EUB05). At the macroscopic level, a total absence of sporulation was observed on all nonhost interactions (Table 1). The apple 'Gala' remained completely symptomless after *V. pyrina* inoculations (Fig. 1C). This is similar to the observation of Chevalier et al [9] after inoculation of 'Gala' with another *V. pyrina* strain. On the contrary, pear plants inoculated with *V. inaequalis* presented frequent pin points symptoms (Fig. 1A) and occasional chlorotic lesions (Fig. 1B). Chlorotic lesions had already been observed by Chevalier et al [9] after inoculation of the pear 'Pierre Corneille' with the *V. inaequalis* strain EUB04, but pin points had never been reported in this nonhost interaction. According to our observations, apple nonhost resistance could be classified as type I and pear as type II according to Mysore and Ryu [11] definition based on the absence/presence of visible HR reaction.

Table 1: Scab qualitative note of pear and apple lines inoculated with *V. pyrina* and *V. inaequalis.* .

Percentage of plants in the different classes of symptoms, 42 days after inoculation				
Class of symptoms	*V. pyrina* strain VP102		*V. inaequalis* strain EUB05	
	'Conference'	'Gala'	'Conference'	'Gala'
0	0	100	90	0
1	0	0	5	0
2	0	0	5	0
3a	0	0	0	0
3b	0	0	0	0
4	100	0	0	100

Class 0: absence of symptoms
Class 1: hypersensitivity (pin points)
Class 2: resistance (chlorotic lesions, slight necrosis, crinkled aspect)
Class 3a: weak resistance (necrotic or chlorotic lesions with occasional very light sporulation)
Class 3b: weak susceptibility (clearly sporulating chlorotic or necrotic lesions
Class 4: susceptibility (sporulation only)

At the microscopic level, three days after inoculation, there was no clear difference between host and nonhost interactions: the conidia of *V. inaequalis* and *V. pyrina* germinated equally on both hosts forming one or two appressoria (Fig. 1 D and F). However, 14 days after inoculation, there was a clear reaction of the plant cells in contact with the appressoria (accumulation of red autofluorescent compounds and enlargement of these cells), which could indicate very small scale hypersensitive reactions (HR) reactions (Fig. 1 E and G) in both plant species. No formation of subcuticular stroma and no conidiogenesis were observed in the nonhost interactions, contrary to the host-resistance reactions [12]. These observations are similar to the collapsed cells described by Chevalier et al [9] in apple and pear nonhost reactions, and to the rare HR-like reactions observed by Stehmann et al [5] on apple inoculated by *V. pyrina*.

Our results indicate that the leaf surface morphology of apple and pear is equally compatible with *V. pyrina* and *V. inaequalis* conidia germination, without specific inhibition at this stage. Recognition probably occurs only at the appressorium site, leading to the cellular reactions observed. These reactions were limited to a few cells without visible symptoms in apple / *V. pyrina* interaction, but extended and produced macroscopic symptoms in pear / *V. inaequalis* interaction.

Different patterns of global gene expression in nonhost resistance in pear versus apple

Differentially expressed genes (DEGs) were analyzed by comparing transcript abundance in leaves between T0 and 24 hours post inoculation (hpi) and between T0 and 72hpi, in the nonhost interactions 'Gala' / *V. pyrina* VP102 and 'Conference' / *V. inaequalis* EUB05. In total, 60 DEGs in apple and 1857 DEGs in pear were identified, which amounts to 0.19 % of all apple genes on the apple AryANE v2.0 microarray, and 4.23 % of all pear genes on the Pyrus v1.0 microarray (Table 2).

Table 2. Number of DEGs identified during apple and pear nonhost response to *V. pyrina* and *V. inaequalis*

	'Gala' / VP102		'Conference' / EUB05	
	24hpi	72hpi	24hpi	72hpi
Total # of DEGs*	49	11	1570	364

DEGs in % of all genes on the microarray**	0.16	0.03	3.58	0.83
% upregulated DEGs	67.3	36.4	74.5	25.5
% of downregulated DEGs	32.7	63.6	25.5	74.5
% of DEGs without TAIR name	27.1	30.4	0.70	1.09

*: DEGs numbers were calculated using the p-adj values ≤ 0.01 as selection threshold

**: 31311 genes on the apple Ariane V2 microarray, 43906 genes on the pear V1 microarray

The very small number of DEGs detected in the apple nonhost interaction at 24 or 72hpi is in agreement with the total absence of macroscopic symptoms observed during this interaction. However, at the microscopic level, small HR-like reactions were detected in the apple / *V. pyrina* interaction. Because theses reactions involve only a few cells in the leaves, the changes in gene expression are probably below the threshold of DEG detection applied in this experiment.

On the contrary, the number of DEGs detected during the pear / *V. inaequalis* interaction is in the same order of magnitude as the number of DEGs detected during pear host resistance to *V. pyrina* (see [12]). This is in agreement with the frequent observation of macroscopic symptoms of resistance (chlorotic lesions or pin points) in this interaction. Among the 1857 pear DEGs, 80.2 % were only detected at 24hpi and 15.4 % only at 72hpi, whereas 4.2 % were upregulated or down regulated similarly at both time points of the kinetics. Among all the pear DEGs observed at 24 and 72hpi, the proportion of up-regulated DEGs was higher (68.8 %) than the proportion of downregulated DEGs (31.2 %). Using MapMan to map the DEGs TAIR names, we observed that the main functional categories represented in this set of DEGs were similar to those observed during pear host resistance to *V. pyrina* (see [12]): protein, RNA, signaling, transport and cell cycle (Fig. 2).

To basically validate the transcriptomic data, 12 DEGS with varied ratios (between -1.9 and 2.9) have been tested in QPCR (Table S1), on the two biological repeats used for transcriptomic analyses. Considering the weak number of DEGs found for apple in this study, we only tested two of them in QPCR. As seen in Table 2 for pear, at 24hpi, a majority of DEGs are up-regulated and at 72hpi, a majority of DEG are down-regulated. QPCR was then performed essentially on DEGs with positive

ratios at 24phi and negative ratios at 72hpi (Table S1). The QPCR results confirmed the induced or repressed status of all tested DEGs.

Weak involvement of hormone signaling pathways classically associated to resistance

Pear DEGs were found that indicate that the jasmonic acid (JA) pathway was repressed. The JA biosynthesis and metabolic conversions were reviewed by Wasternack et al [13]. In our data, at 24hpi, the first step of JA biosynthesis, that is the conversion of linoleic acid in 12-oxo-phytodienoic acid (OPDA), is compromised given the repression of six about seven lipoxygenases (LOX) (three LOX1, two LOX2 and two LOX5), the last one being induced (Fig. 3). OPDA produced in the chloroplast is then transported to the peroxisome for subsequent conversion to JA via the action of OPR3 (12-oxo-phytodienoic acid reductase) and β-oxidation enzymes (reviewed in [14] and in [13]). In pear, three β-oxidation enzymes were found activated more or less rapidly: ACX4 (24hpi), MFP2 (72hpi) and the thioesterase homolog to *At2g29590* (72hpi), which suggests that constitutive OPDA stocks were turned into JA. But the early and long-lasting induction of *JMT* and *ST2A* genes is in favor of a rapid conversion of JA in inactive compounds, *JMT* induction being reinforced by *BBD1* repression (24hpi). *BBD1* is actually known as a negative regulator of *JMT* [15].

The defense response depending on JA was also clearly repressed in pear (Fig. 3). The transcription activator MYC2 of JA-induced genes is known to be repressed by its interaction with JAZ proteins (reviewed in [13]), and two *JAZ1* and one *JAZ3* coding genes were found activated at 24hpi in pear. UBP12 is known as a stabilizer of MYC2 [16]. In our data, *UBP12* was found repressed at 72hpi, which reinforces the inactivation of MYC2. WRKY33 is known as an activator of the JA defense pathway [17] and WRK70 [18] or AS1 (or MYB91; [19]) as inhibitors, and among JA-responsive proteins, the pathogenesis-related PR3, PR4 and PR12 act downstream MYC2 activation [20]. In our data, accordingly with the repression of the activator WRKY33 and the activation of the inhibitors WRK70 and AS1, some JA-responsive genes were also found repressed, such as the chitinase coding genes *PR4* (also called *HEL*) and *ATEP3*. Furthermore, no DEGs were found for PR3 and PR12 functions. To

conclude, in the nonhost interaction between pear and *V. inaequalis*, some JA seems to be produced, but rapidly converted in inactive compounds and the subsequent defense response is clearly repressed.

Pear DEGs were found that seems to indicate that the salicylic acid (SA) pathway was slightly engaged and rapidly repressed (Fig. 3). *WRKY70* was induced at 72hpi in our data. This transcription factor is known as a negative regulator of SA biosynthesis but a positive regulator of SA-mediated defense genes in Arabidopsis ([21]; [22]; [23]), among them *PR2*, *PR5* but not *PR1* [24]. *WRKY33* which is known as a negative regulator of SA-responsive genes [25], was also repressed at 72hpi in our data. PR2 and 5 are well-known anti-fungal proteins ([26]; [27]; [28]). At 24hpi a *PR2*, two *PR2-like*, a *PR5* and a *PR5-like* coding genes were found induced in our work, another *PR2-like* and two others *PR5-like* being repressed. The differential expression was maintained at 72hpi for only two of the activated ones. Furthermore no DEG was found for the PR1 function but three *PR1-like* genes were found repressed: *ATPRB1* and genes homolog to *At5g57625* and *At4g33720*. *ATPRB1* was already reported as repressed by SA treatment [29]. In our data, the WRKY70 transcription factor was induced later than the induced PR genes so we could imagine that induced PR genes were activated by another precocious regulation, such as an oxidative burst (see below), rather than by WRKY70. Furthermore, WRKY70 induction seems not sufficient to enable a long lasting induction of these defense genes.

SA accumulation was also rather mixed. *CBP60a* [30], *ACA11* [31], *EICBP.B* (or *CATMA1*; [32]), all three coding calcium-sensor proteins, are known as negative regulators of SA accumulation and biosynthesis, as well as the light signaling factor *FAR1* [33] or the SA glucosyltransferase *UGT74F1* which convert SA in inactive SA 2-O-beta-D-glucoside or the glucose ester of SA [34]. On the contrary *EDS1*, *PAD4* (reviewed in [35]) and *MKS1* [36] are known as positive regulators of SA accumulation. In our data, the repression of *CBP60a*, *ACA11* and *EICBP.B* genes sustained a SA biosynthesis and accumulation. In addition, *EDS1* activation allowed to consider a positive feedback loop likely to potentiate SA action via EDS1 cytosolic homodimers, even though *PAD4* was repressed. But, as well

as *WRKY70* induction, the repression of the MAPK *MKS1* and the activation of the light signaling factor *FAR1* (2 times) or the SA glucosyltransferase *UGT74F1* were in favor of less free SA. Concerning SAR, *MES1* is known as required in healthy systemic tissues of infected plants to release the active SA from methyl-SA, which serves as a long-distance signal for systemic acquired resistance (SAR) [35] and *ACBP6* may be involved in the generation of SAR inducing signal(s) [37]. In our data, SAR seemed compromised given the repression of *ACBP6* at 24hpi and *MES1* at 72hpi.To conclude, in the nonhost interaction between pear and *V. inaequalis*, the SA pathway could be engaged but transiently and presumably reduced to the few infection sites and not spread by SAR in healthy systemic tissues.

Calcium influx and reactive oxygen species (ROS) production act as secondary messengers and lead to stomatal closure

Early responses of plants upon pathogen perception include calcium influx and ROS production, which both act as secondary messengers ([38], reviewed in [10]). Three pear DEGs were found that indicate early increased cytosolic calcium level. The CSC (Calcium permeable Stress-gated cation Channel) ERD4 (found two times) and the two glutamate receptors GLR3.4 and GLR2.7, are known as calcium permeable channels ([39]; [40]). They were induced at 24hpi in our data. An increased cytosolic calcium level can lead to a pre-invasive defense response by stomatal closure and promote the post-invasive defense response ROS accumulation [41].

Calcium influx has been reported to promote stomatal closure through the regulation of potassium flux and the activation of anion channels in guard cells (reviewed in [10]). The stomata closure is known to be induced via the inhibition of inward potassium currents which is achieved via activation of calcium dependent protein kinases (CDPK) such as CPK13 and CPK8/CDPK19 ([42]; [43]); but also via activation of CBL1 of the CBL1-CIPK5 complex, which activates the GORK potassium outward channel [44]. CPK13, CPK8/CDPK19 and CBL1 were all activated at 24 hpi in our data.

A NADPH oxidase *RBOHB* (respiratory burst oxidase homologs, RBOH) is early and long-lasting induced in the pear/*V. inaequalis* nonhost interaction suggesting a rapid and maintained apoplastic

ROS production. Indeed, the apoplastic ROS are mainly produced by plasma membrane localized NADPH oxidases, cell wall peroxidases and amine oxidases [45]. In addition, posttranslational regulation of RBOH is required for its activation and ROS production. Calcium, phosphatidic acid, and direct interactors such as Rac1 GTPase and RACK1 (Receptor for Activated C-Kinase 1) have been reported to be positive regulators of RBOHs (reviewed in [46]). For example, the Rac-like/ROP GTPase ARAC3 is known to interact with a RBOH to promote ROS production [47]. In our data, RBOHB activity was also supported by the presence of positive regulators such as Rac-like/ROP GTPase. The three Rac-like/ROP GTPase *ARAC1*, *ARAC3* and the homolog of *At4g03100* were induced at 24hpi. CDPKs such as CPK1 are also known to activate RBOHs in response to increased cytosolic calcium level [48]. But repression of *CPK1* in our data seems to indicate that this way of activation did not function.

In response to abscisic acid (ABA) or microbe-associated molecular pattern (MAMP) immunity, stomatal closure is known to be regulated by apoplastic ROS production (reviewed in [49]) and cysteine-rich receptor-like kinases (CRK) are also known to be elements between ROS production and downstream signaling leading to stomatal closure, sometimes activated (CRK10), sometimes inhibited (CRK2 and CRK29; [50]). Three DEGs coding for CRK were found in our data and the repression of *CRK2* and *CRK29* (found two times) was consistent with the stomata closure previously found, but the repression of *CRK10* (found two times) was not. Beyond closure, inhibition of stomatal development could be seen as an extreme defense. YODA (found two times) and MPK6 (found two times) MAPKs belong to a pathway involved in the negative regulation of stomata development [51]. These two genes were early induced in our data.

To conclude, in pear/*V. inaequalis* nonhost interaction, a calcium influx leads to the development of the stomatal closure pre-invasive defense, but also promotes a post-invasive defense: apoplastic ROS accumulation. Apoplastic ROS, acting themselves as messengers, come to strengthen the stomatal closure (Fig. 4).

Transcription factors and sphingolipids maintain HR under control

ROS are known to mediate cellular signaling associated with defense-related gene expression, hypersensitive response (HR) i. e. the programmed cell death (PCD) at the site of infection during a pathogen attack, and phytoalexin production [52]. *Arabidopsis thaliana* RCD1 regulator has been proposed to positively regulate cell death in response to apoplastic ROS by protein-protein interactions with transcription factors (reviewed in [53]) and WRKY70 and SGT1b were identified as cell death positive regulators functioning downstream of RCD1 [53]. *RCD1* and *WRKY70* genes were found induced in our data, at 24hpi and 72hpi respectively.

In Arabidopsis, the F-box protein CPR1, in association with the Skp1-Cullin-F-box (SCF) ubiquitin ligase complex, targets for degradation NLR (nucleotide-binding domain and leucine-rich repeats containing proteins) resistance protein such as SNC1, RPM1 or RPS2, to prevent overaccumulation and autoimmunity (reviewed in [54]). A *Skp1-like* (*ASK19*; 72hpi) gene and *CPR1* (24hpi) gene were found induced in our data. A gene coding for RPM1 function was also found repressed at 24hpi. These results are in favor of the hypothesis that NLR receptors do not take part in the HR development observed in the pear/*V. inaequalis* nonhost interaction (Fig. 1A). In addition, the induction of an *AtSerpin1* gene homolog at 24hpi (found two times) in our data is consistent with that hypothesis. Indeed, AtMC1 is a pro-death caspase-like protein required for full HR mediated by intracellular NB-LRR immune receptor proteins such as RPP4 and RPM1 [55] and AtSerpin1 is a protease inhibitor which block AtMC1 self-processing and inhibit AtMC1-mediated cell death [56].

The differential expression of two others components of the proteasome pathway is in favor of an HR development: the induction of the *RIN3* ubiquitin E3 ligase (24hpi) and the repression of the *BRG3* ubiquitin E3 ligase (24hpi). Indeed, RIN3 is known as positive regulator of RPM1 dependent HR [57]. And BRG3 is known as a negative regulator of HR in plant/necrotrophic pathogen interactions [58].

Sphingolipids are involved in the control of PCD, either as structural components of membranes but also as initiators in the cell death regulatory pathway. According to Huby et al [59], free ceramides and long chain/sphingoid base components (LCBs) are able to trigger cell death, via ROS production,

whereas their phosphorylated counterparts, ceramide phosphates and long chain base phosphate components (LCB-Ps) promote cell survival. The induction of PCD by LCB is based on the activation of protein kinases, among them MPK6 [60]. As already mentioned, *MPK6* was found early induced in our data and we found numerous DEGs in the nonhost interaction between pear and *V. inaequalis* that indicate the presence of free ceramides and LCB, which possibly participate to the HR development. Free LCB presence is demonstrated by the activations of *SBH1* (24hpi), *SLD1* (24hpi) and another sphingolipid Δ8 long-chain base desaturase homolog to *At2g46210* (24hpi; found two times), and their relative conversion in ceramides is demonstrated by the differential expressions of the ceramide synthases *LOH2* (repressed at 24hpi) and *LOH3/LAG13* (induced at 24 and 72hpi). LCB non-conversion in phosphorylated counterparts is shown by the *AtLCBK1* repression (72hpi) and free ceramides maintenance is attested by their non-conversion in glycosyled ones given the repression of a glucosyl ceramide synthase homolog to *At2g19880* (24hpi).

The differential expression of numerous known regulators of HR in our data is again consistent with the HR phenotype observed. The mechanosensor MSL10 and the calmodulin-activated Ca^{2+} pump (autoinhibited Ca^{2+}-ATPase [ACA]) ACA11 were found engaged: at 24hpi *MSL10* was induced and *ACA11* was repressed. MSL10 is known as a positive regulator of cell death [61] and ACA11 is known as a negative regulator of SA-dependent programmed cell death [31]. Their modulation is linked with the noticed calcium influx discussed above ([31]; [62]). The participation of the SA pathway in the development of the hypersensitive response could also be supported by the repression of *EDR1* (at 72hpi). Indeed, the MAPKKK EDR1 is known as a negative regulator of the SA-dependent HR (reviewed in [63]).

Three other regulators of HR were found modulated in our data. The transcription factor *AS1* (*MYB91*) was found induced at 24hpi. It is known as a positive regulator of HR and implicated in JA pathway (reviewed in [18]). The transcription factor *WRKY40* was found repressed at 72hpi. It is known as a negative regulator of HR [64] and implicated in PTI [65]. Another negative regulator of HR is the lipid-binding domains containing protein VAD1 [66]. It was found repressed at 72hpi.

303 The behavior of two others genes in our data seems to indicate that the developed HR was contained
304 and not carried away due to too much intracellular ROS production and damages. The function
305 *UGT73B3* and *CAT2* were thus activated (24hpi). UGT73B3 and CAT2 are known as restrictors of HR
306 expansion via their action in ROS scavenging (CAT2; [67]) or in detoxification of ROS-reactive
307 secondary metabolites (UGT73B3; [68]).
308 To conclude, in pear/*V. inaequalis* nonhost interaction, HR was spread out, in link with the calcium
309 influx, but especially following apoplastic ROS production and ROS production via free sphingolipids
310 accumulation and not via NLR receptors. Furthermore, the behavior of not less than height regulators
311 indicate that the developed HR is under control (Fig. 4).
312
313 Cell wall carbohydrates content and cuticle composition are altered
314
315 The first obstacle encountered by host as well as nonhost pathogens attempting to colonize plant
316 tissues is the plant cell wall, which is often covered with a cuticle. Preinvasive penetration barrier, as
317 a preformed physical barrier, or as the onset place of defensive signaling pathways, is considered an
318 important factor, especially in nonhost resistance in which non adapted pathogens normally fail to
319 penetrate nonhost plant cells when blocked by the cell wall ([10]; [41]). Plant cell wall alterations, of
320 the carbohydrates or the phenolic components, either by impairing or overexpressing cell wall-
321 related genes, have been demonstrated to have a significant impact on disease resistance and/or on
322 abiotic stresses (reviewed in [69] and [70]).
323 We found numerous genes related to the cell wall with a modified expression during nonhost
324 interaction between pear and *V. inaequalis*, among them about thirty related to the biosynthesis or
325 the modification of carbohydrates. These genes are presented in table 3, except those related to the
326 lignin and other phenolic compounds, which will be discussed later. We saw in particular several
327 genes related to cellulose (8) and even more genes related to pectin (14) but no genes related to
328 callose.

329 Concerning these particular carbohydrate components, the model proposed by Bacete et al [69] is as
330 follows. Firstly, alterations in cellulose biosynthesis from primary or secondary cell wall trigger
331 specific defensive responses, such as those mediated by the hormones JA, ET or abscisic acid (ABA),
332 activate biosynthesis of antimicrobial compounds, but also might attenuate pattern triggered
333 immunity (PTI) responses. Secondly, alterations of cell wall pectins, either in their overall content,
334 their degree of acetylation or methylation, activate specific defensive responses, such as those
335 regulated by JA or SA, and trigger PTI responses, probably mediated by damage-associated molecular
336 patterns like oligogalacturonides. Thus, even though our results do not completely support a role of
337 these genes, we think that the modified expression of cell wall related genes during nonhost
338 interaction between pear and *V. inaequalis* is meaningful.
339
340
341 **Table 3: Main DEGs related to cell wall carbohydrates synthesis/modification detected during non-**
342 **host interaction pear/*V. inaequalis*.**
343

	Gene	Action	Expression*
		Primary cell wall	
Cellulose	*CSLA2*	synthesis	I
	PNT1	synthesis	I
	COBL2	deposition (GPI-anchored protein)	R
	AtGH9A4	catabolism	I
	XTR7	loosening	I
Hemi-cellulose (xyloglucan)	*At5g15490*	synthesis	I
Pectin	*At3g42180*	synthesis	I
	At4g01220	synthesis	I
	GHMP kinase	synthesis	I
	RHM1	synthesis	R
	PME At2g45220	methylesterification	I
	PME At2g46930	methylesterification	I
	PME At3g05910	methylesterification	R
	PME At1g02810	methylesterification	R
	PME44	methylesterification	R

	PG At3g16850	depolymerisation	I
	PG At3g59850	depolymerisation	I
	PG At4g13710	depolymerisation	I
	PG At3g62110	depolymerisation	R
	IDA	degradation	R
Arabinogalactan protein	*AGP11*	_	I
	AGP1	_	R
Secondary cell wall			
Cellulose	*CESA09*	synthesis	I
	CESA10	synthesis	I
	CSLG1	synthesis	I
Hemi-cellulose (xylan)	*FRA8*	synthesis	I
Undetermined			
Expansin	*EXP15*	loosening	I
	EXPB3	loosening	I
Hemi-cellulose	*ATFUC1*	modification	I
	XTH33	growth and assembling	R

*I: induced, R: repressed

Concerning the cuticle layer, most cuticles are composed largely of cutin, an insoluble polyester of primarily long-chain hydroxy fatty acids. This lipophilic cutin framework is associated with hydrophobic compounds collectively referred to as waxes. The cuticle is also thought to contain varying amounts of intermingled cell wall polysaccharides and sometimes also a fraction termed cutan (reviewed in [71]). Cutin monomers are synthesized by the modification of plastid-derived 16C and 18C fatty acids in the endoplasmic reticulum (ER), yielding variously oxygenated fatty acid–glycerol esters referred to as monoacylglycerols, which polymerize upon arrival at the growing cuticle (Fig. 5, reviewed in [71]).

C16 and C18 fatty acids are also important precursors of cuticular wax synthesis (Fig. 5). Upon transport to the ER, the C16 and C18 fatty acids are extended to form very-long-chain fatty acids (VCLFAs; C>20), and this extension is carried out by the fatty acid elongase (FAE) complex located on the ER membrane. The very-long-chain FAs are then converted into the varied cuticular waxes (primary alcohols, aldehydes, alkanes, secondary alcohols, ketones) by many ways (reviewed in [72]). Interestingly, we found three genes upregulated 24hpi belonging to the FAS (fatty acid synthase) chloroplastic complex implicated in the production of the C16 precursor (Fig. 5): *ACCD*, *FabG* and

MOD1 (found two times). ACCD encodes the carboxytransferase beta subunit of the Acetyl-CoA carboxylase complex which catalyzes the first committed step in fatty acid synthesis: the carboxylation of acetyl-CoA to produce malonyl-CoA. FabG and MOD1 are respectively a β-ketoacyl ACP-reductase and an enoyl-ACP-reductase which catalyze respectively the conversion of acetoacetyl-ACP into β-hydroxyacyl-ACP and the second reductive step from enoyl-ACP to butyryl-ACP (reviewed in [72]).

In the ER, the four functions we found related to waxes biosynthesis in our data were repressed at 24hpi: *KCS4* (found two times), *CER1* and *CER3*, or 72hpi: *ECR/CER10*. KCS4 and ECR/CER10 belong to the FAE complex ([73]; [74]). The last two genes are implicated in aldehydes (*CER1*) and alkanes (*CER1 and 3*) generation (reviewed in [72]). On the contrary, the eight genes we found connected to cutin biosynthesis were induced at 24hpi except a gene homolog to *At5g14450*, which was induced at 72hpi. One of them is a glycerol-3-phosphate acyltransferase (GPAT) coding gene: GPAT8, which catalyzes the transfer of a fatty acid from coenzyme A (CoA) to glycerol-3-phosphate (Fig. 4; reviewed in [71]). GPAT8 function in cutin formation has been functionally confirmed in association with GPAT4 [75]. The seven others genes code GDSL-lipases enzyme (*At1g28600*, *At1g28660*, *At1g54790*, *At3g16370*, *At3g48460*, *AtCUS4*: *At4g28780*, *At5g14450*), some of which have been shown to function as cutin synthase (Fig. 4; [76]; reviewed in [71]) and polymerize monoacylglycerols.

We also found induced respectively at 24 and 72hpi two genes involved in waxes and cutin biosynthesis positive regulation: *MYB16* and *SHN1*. The SHN genes (*SHN1–SHN3*), a set of three largely redundant APETALA 2 family transcription factors from *A. thaliana*, are regulators of floral cutin and epidermal cell morphology. SHN1 is regulated by the MYB family transcription factor MYB106, which, along with its paralog MYB16, controls many aspects of cuticle and epidermis formation in *A. thaliana* (reviewed in [77] and [71]).

Cutin and cuticular waxes play an important role in plant-insect and plant-microbe interactions. Numerous Arabidopsis mutants in cutin and waxes biosynthetic or transport genes, such as Acyl-CoA binding proteins (ACBP), show varying degrees of cuticle impairment, alterations in cutin and/or wax

composition, and defects in SAR (reviewed in [72]). We found *ACBP6* repressed at 24hpi. That repression is not inconsistent with the previously described amplification of cutin biosynthesis and polymerization, given that *acbp6* KO mutation is not associated with a defect in that pathway [37]. That repression is also consistent with the SAR repression observed above as the *acbp6* KO mutant show compromised SAR [37].

To conclude, our analysis of nonhost pear/V. *inaequalis* interaction identified an alteration of the cuticle composition with more cutin and less waxes synthesis. The increase in cutin polymerization could lead to a thickening of the cuticular layer to prevent fungus penetration via its appressoria.

Secondary metabolism leads to G unit lignin polymerization and simple coumarin or hydrocinnamic acid amine phytoalexins synthesis

As distinguished from primary metabolism, plant secondary metabolism refers to pathways and small molecule products of metabolism that are non-essential for the survival of the organism. But they are key components for plants to interact with the environment in the adaptation to both biotic and abiotic stress conditions. Plant secondary metabolites are usually classified according to their chemical structure. Several groups of large molecules, including phenolic acids and flavonoids, terpenoids and steroids, and alkaloids have been implicated in the activation and reinforcement of defense mechanisms in plants (reviewed in [78]).

Terpenoids and steroids, or isoprenoids, are components of both the primary and secondary metabolisms in cells, and mono-, tri-, sesqui- and polyterpenes are considered as secondary metabolites (reviewed in [79]). Our results on pear identified seven DEGs and five DEGs belonging to the chloroplastic methylerythritol posphate (MEP) and to the cytosolic mevalonic acid (MVA) pathway of isoprenoids production respectively (Table 4), which results, among others compounds, in tri- and sesquiterpenes secondary metabolites. The majority of these genes contribute to produce primary metabolites according to Tetali [79]. Except *SMT2*, that we found induced at 24hpi, there is no report concerning a putative implication of others genes in plant biotic resistance. SMT2 is

involved in sterols production and *smt2* mutation was reported to compromise bacterial resistance in *Nicotiana benthamiana* [80]. The hypothesis is that sterols regulate plant innate immunity against bacterial host and nonhost infections by regulating nutrient efflux into the apoplast. *V. inaequalis* is an hemi biotrophic pathogens which colonizes only the apoplast compartment since the beginning of the interaction. *SMT2* strong relative induction in our data could indicate that a similar mechanism of nutrient efflux regulation via sterols could take place to limit the fungus growth in pear nonhost resistance against *V. inaequalis*.

Table 4: Main DEGs involved in biosynthetic pathways for terpenes and isoprenoids during pear/*V. inaequalis* non-host interaction.

	Gene	Function	Expression*
Cytosolic MVA (mevalonic acid) pathway enzymes	*HMGS*	catalyze the second step of the pathway	R
	HMGR1	catalyze the third step of the pathway	R
	SMT2	sterols production	I
	FLDH	sesquiterpenes production	R
	SQE2	triterpenes production	I
Chloroplastic MEP (methylerythritol posphate) pathway enzymes	*DXR*	catalyzes the second step of the pathway	I
	GG reductase	chlorophylls production	R
	VTE4	tochopherols production	I
	KAO1	gibberellins production	R
	PDS2	plastoquinones production	I
	LYC	carotenoids production	I
	PGGT1	covalent attachment of a prenyl group to a protein	I

In our data, the other DEGs that were linked to the secondary metabolism belong to the phenylpropanoid pathway production (Fig. 6). Among them we found four genes belonging to the flavonoid production, all repressed, at 24hpi (*DFR* and *DRM6*) or 72hpi (*TT7* and *UGT71D1*). DFR (dihydroflavonol reductase) is involved in flavan-3,4-ol production and TT7 (flavonoid 3' hydroxylase) in dihydroquercetin production from dihydro-kaempferol, and UGT71D1 (glucosyl transferase) in quercetin-glycoside production from quercetin (TAIR database;

https://www.arabidopsis.org/index.jsp). DMR6 (flavone synthase) is involved in flavone production from naringenin [81]. Thus flavonoid production does not seem to be favored, which is not consistent with the induction of *MYB12* at 24hpi, but consistent with *MYB4* induction at 72hpi. MYB12 is actually known as a positive regulator of flavonol biosynthesis in pear and apple fruits ([82]; [83]) whereas MYB4 is known as a negative regulator of this biosynthetic pathway [84].

Concerning the production of monolignols, precursors of lignin synthesis, some genes were found induced, others repressed. We found *CYP98A3* and *CAD9* (found two times) induced at 24hpi and *HCT*, *CCR1* and a gene homolog to *At2g23910* (found two times, one time repressed at 72hpi) repressed at 24hpi Fig. 6). *CYP98A3* encode a C3H (coumarate 3-hydroxylase), *CAD9* encode a CAD (cinnamyl alcohol dehydrogenase), HCT is an hydroxycinnamoyl-CoA shikimate/quinate hydroxycinnamoyl transferase, *CCR1* encode a CCR (cinnamoyl-CoA reductase) and *At2g23910* encode a CCR-related protein. (TAIR and KEGG databases (https://www.genome.jp/kegg/)).

Lignification is obtained by cross-linking reactions of the lignin monomers or by polymer–polymer coupling via radicals produced by oxidases such as peroxidases [85] and laccases [86]. However, while peroxidases are able to oxidize monolignols to produce H, G and S units of lignin, laccases only generate G units [85]. In our data, we found two laccases induced at 24hpi: *LAC11* (found two times, one time induced at 24 and 72hpi) and *17* (found two times), and three peroxidases repressed at 24hpi: *PRX17*, *PER47* and *PRX52* (also repressed at 72hpi), which can be linked to lignin biosynthetic process (Fig. 6). According to Zhao et al. [86], LAC11 and 17, along with LAC4, play a critical role in lignification, and their results suggests that peroxidase and laccase do not serve redundant functions in lignification, at least in the vascular tissues of the stem and root of Arabidopsis. Participation in lignin formation has also been proved for PRX17 [87], PER47 [88] and PRX52 [89]. But there are currently no reports about a possible involvement of all these genes in lignification linked to biotic or abiotic stresses. Concerning non-host resistance, two reports describe lignin accumulation/deposition involvement: one in apple fruit [90] and the other one in cowpea [91]. In the latest, authors showed that preferentially generated lignin units in this nonhost interaction are G

457 units, just as it seems to be the case in our pear / *V. inaequalis* study. To summarize, it is tempting to
458 think that modifications of expression observed for genes linked to lignin polymerization are relevant
459 for the pear nonhost resistance against *V. inaequalis*, but further functional analysis should be
460 conducted to conclude.
461 The biosynthesis of two others types of phenylpropanoid compounds appears to be favored during
462 pear nonhost resistance against *V. inaequalis*: simple coumarin on one hand and hydroxycinnamic
463 acid amides on the other hand. We found four *BGLU*-like genes induced at 24hpi: *BGLU42* (also
464 induced at 72hpi), *47* and *BGLC3*, or 72hpi: *BGLU16* (Fig. 6). These β-glucosidases could be implied in
465 simple coumarin path production from the cinnamic acid (KEGG database). Some natural simple
466 coumarins are known as antifungal compounds *in vitro* and have been developed as fungicides [92].
467 Ancient work on Hevea also reports the correlation between the resistance against pathogenic fungi
468 and the production of some coumarins, with antifungal activity *in vitro* [93]. We also found induced
469 at 24hpi the genes *AACT1/ACT1*, *ATPAO5* and genes homologs to *At4g17830* and *At4g38220* (Fig. 6).
470 AACT1/ACT1 catalyze the first specific step in branch pathway synthesizing hydroxycinnamic acid
471 amides from the p-Coumaroyl CoA or the feruloyl CoA and amines agmatine or putrescine [94].
472 Hydroxycinnamic acid amides are produced in response to pathogenic infections [94] and surface
473 exported. Hydroxycinnamic acid amides are reported to participate in Arabidopsis nonhost resistance
474 against *Phytophthora infestans* via their inhibitory activity on spore germination [95]. The three
475 others genes belong to the arginine biosynthesis path (homologs to *At4g1783* and *At4g38220*) and
476 the arginine and proline metabolisms which produce the amines agmatine and putrescine (*ATPAO5*)
477 (KEGG database). Agmatine is directly produced from arginine thanks to an ADC activity (arginine
478 decarboxylase) and putrescine can be produced from spermidine thanks to a PAO activity (polyamine
479 oxidase). ATPAO5 catalyzes the conversion of spermine in spermidine. The induction of these three
480 last genes is therefore consistent with the hypothesis of amines production in order to enable
481 hydroxycinnamic acid amides synthesis. The induction of *C4H* at 24hpi could also favor
482 hydroxycinnamic acid amides synthesis via p-Coumaroyl CoA biosynthesis promotion. C4H

(cinnamate 4-hydroxylase) catalyzes the production of p-Coumaric acid from Cinnamic acid and p-Coumaric acid gives p-Coumaroyl CoA thanks to 4CL (4- coumarate-CoA ligase) (KEGG database).

Among the suite of defense components synthetized in nonhost as in host context, a chemical barrier can be established via accumulation of a diverse array of secondary metabolites rapidly produced upon pathogen infection, named phytoalexins, with toxic or inhibitory effects (reviewed in [10]). Phytoalexins can be flavonoids, such as the pisatin of pea (in [96]) but also varied phenylpropanoid compounds. In the nonhost interaction pear / *V. inaequalis*, the production of flavonoid type phytoalexins does not seem to be favored, except simple coumarin and hydroxicinnamic acid amines.

Very limited transcriptomic modulation during apple / *V. pyrina* nonhost interaction

Only 60 DEGs were detected in the apple / *V. pyrina* nonhost interaction at 24 or 72hpi, in agreement with the total absence of macroscopic symptoms and few cells engaged in an HR-like reaction observed at the microscopic level. Among these 60 DEGs, 36 have no known function. Among the 24 remaining DEGs, nine DEGS could be relevant in apple / *V. pyrina* nonhost interaction in view of our findings in pear / *V. inaequalis* nonhost interaction. *ORG2* (*BHLH038*), a putative integrator of various stress reactions [97] was induced at 24hpi. Three genes were related to an oxidative stress: *GASA10* was repressed at 24hpi and *NRAMP3* and *AOR* were induced at 24hpi. GASA proteins have been suggested to regulate redox homeostasis via restricting the levels of $OH^{\cdot}$ in the cell wall [98]. The repression of this gene is thus in favor of more $OH^{\cdot}$ in the cell wall. The oxidoreductase coding gene *AOR* is known in the chloroplast to contribute to the detoxification of reactive carbonyls produced under oxidative stress [99]. *NRAMP* genes function as positive regulators of ROS accumulation, especially during Arabidopsis *Erwinia chrisanthemi* resistance [100]. The induction (at 24 and 72hpi) of another gene suggests modifications at the cell wall level: *EXP8*, an expansin coding gene involved in cell wall loosening (Tair database). We also found two genes related to hormone pathways, one induced at 24hpi: *WIN1* and the other one repressed at 72hpi: *UBP12*. WIN1 is known as a negative regulator of SA pathway [101] and UBP12 as a positive regulator of JA pathway via the stabilization of

MYC2 [16]. In link with the JA pathway, we also found *TPS21* induced at 24hpi. TPS21 is involved in sesquiterpenes production and is promoted by JA signal via MYC2 [102]. TPS21 is especially involved in the jasmonate-dependent defensive emission of herbivore-induced volatiles in cranberries [103]. Finaly the last DEG we found relevant in apple / *V. pyrina* nonhost interaction could promote HR via ceramides accumulation. *ACD11* is repressed at 24hpi in our data. In *acd11* mutants, the relatively abundant cell death inducer phytoceramide rises acutely [104].

Because nonhost resistance of apple against *V. pyrina* is of a type I, with a very limited number of cells engaged in an HR-like reaction, it has not been possible for us to exhaustively describe how this interaction is expressed at the transcriptomic level. Further insight with more adapted technics such as laser-assisted cell picking, prior to micro arrays or RNA sequencing analysis (review in [105]) could provide more information in the future.

Comparison of pear resistances against the host pathogen *V. pyrina* and the nonhost pathogen *V. inaequalis*

Perchepied et al [12] performed a detailed transcriptomic analysis of the host resistance of pear against *V. pyrina* strain VP102, deployed in a transgenic pear bearing the well-known apple *Rvi6* resistance gene against *V. inaequalis*. Comparing this work to our gives us the rare opportunity to analyze similarities and differences between a host and a nonhost resistance in the same plant. Only four transcriptomic studies involving pear/pathogen interactions have been published so far. Yan et al [106] reported the modulation of expression of 144 pear genes after fruit treatment by *Meyerozyma guilliermondii*, an antagonistic yeast used for biocontrol of natural pear fruit decay. Zhang et al [107] similarly reported the modulation of expression of 1076 pear genes after treatment with *Wickerhamomyces anomalus*, another biocontrol agent. Using RNA-seq, Wang et al. [108] reported a major role of ethylene signalization during the compatible interaction between *P. pyrifolia* and *Alternaria alternata*, a necrotrophic pathogen. Finally, Xu et al. [109] applied RNA-seq to

characterize the genes of *Penicillium expansum* activated after infection of pear fruits. None of these studies can be directly compared to our work on host and nonhost scab pear resistance.

Concerning the recognition and early signaling steps of the interactions, many receptors and co-receptors have been found induced in the host pear resistance, especially damage-associated molecular patterns receptors such as RLK7, revealing that PTI and ETI must be engaged. We did not found evidence of the mobilization of such receptors in the pear nonhost resistance. PTI and ETI receptors are nonetheless reported as implicated in nonhost resistance (reviewed in [110] and [10]). As we only analyzed post infection transcriptional modulations in the nonhost pear/*V. inaequalis* interaction (at 24 and 72hpi), one hypothesis to explain the lack of PTI and ETI receptors in our data could be that these receptors were already present as preformed defenses and not particularly induced by the infection onset. In pear nonhost interaction, the earliest signaling pathways we were able to highlight are calcium influx and apoplastic ROS production. Calcium signaling seems to be also implicated in pear host resistance, but less obviously than in nonhost resistance.

About the hormonal signaling pathways, the JA defense signaling pathway was found repressed in pear nonhost resistance but quite activated in pear host resistance. The JA/ethylene (ET) defense signaling pathway is known as an effective defense against necrotrophic fungi in Arabidopsis [111]. Thus, it is not surprising to find the JA pathway repressed in the development of the pear nonhost resistance against the hemi-biotrophic pathogen *V. inaequalis*. But it is very interesting to find this pathway rather induced in the development of the pear host resistance against the other hemi-biotrophic pathogen *V. pyrina*. The SA signaling pathway is commonly seen as the classical one triggered to resist biotrophic fungi in Arabidopsis [111], but only a little engagement in pear nonhost resistance has been observed, SA signaling being repressed in pear host resistance. If this absence of SA implication is quite unexpected in pear host resistance against a hemi-biotrophic fungus, it is consistent with the report that the exact role of these key defense phytohormone is unclear in nonhost resistance and remains to be established [41]. As shown by Tsuda et al [112], an explanation for the hormone pathways behavior in pear host resistance could be that: as both the SA and JA/ET

pathways positively contribute to immunity, a loss of signaling flow through the SA pathway can be compensated by a rerouting signal through the JA/ET pathways. In addition, independently of SA signaling, but in positive connection with JA signaling, SAR seems to be engaged in distal tissues during pear host resistance. To conclude, in pear host as well as nonhost resistances, classical resistance hormones SA and JA/ET, and the correlative PR gene defenses, seems differently involved than in Arabidopsis.

The carbohydrate content of the cell-wall is modified in response to the attacks by the pathogens. Regarding cell-wall and cuticle, in pear host as well as nonhost resistances, important modifications were highlighted. Similar modifications affected the cellulose and mainly the pectin contents, but no callose production was observed. Regarding cuticle, waxes production was induced in host resistance whereas it was repressed in nonhost resistance, in favor of cutin production / polymerization, which was also induced in host resistance. To conclude, as a first obstacle encountered by host as well as nonhost pathogens attempting to colonize plant tissues, the plant cell wall and its cuticle seem to play a foreground role in pear host as well as nonhost resistances.

Finally, the production of secondary metabolites and phenylpropanoids compounds in particular, seems to be a major line of defense, in pear host as well as nonhost resistances, but with divergences. If lignin and flavonoid productions are preponderant in pear host resistance against *V. pyrina*, lignin implication in pear nonhost resistance is less clear and flavonoids production is obviously repressed. But the biosynthesis of two other types of phenylpropanoid-derived phytoalexins appears to be favored during pear nonhost resistance: simple coumarin on one hand and hydroxycinnamic acid amides on the other hand.

The comparative analysis between a host and a nonhost resistance in pear shows that, even though specificities are observed, the two major defense lines engaged are shared: the cell wall and its cuticle on one hand, the secondary metabolism with the phenylpropanoid pathway on the other hand. Moreover, these defenses seem deployed largely independently of the SA signaling pathway, widely recognized as the main defense hormone against biotrophic pathogens.

Conclusion

As far as we know, our work is the first one published regarding a transcriptomic analysis of post-infections events of a nonhost resistance to *Venturia sp.* in apple and pear. Velho and Stadik [113] recently published a detailed description of the apple / *Colletotrichum higginsianum* nonhost resistance, highlighting the accumulation of callose at the sites of penetration of the fungus. But no data on gene expression was included. Here, our molecular work on apple / *V. pyrina* nonhost resistance remains preliminary and in order to allow a deeper deciphering, further analyses must be considered with the aid of tools adapted to this type I nonhost resistance with very few cells engaged in an HR-like reaction, only visible at a microscopic level. In pear, this deciphering allowed us to show that nonhost resistance against *V. inaequalis* is a type II one, which involves enough pathogen penetration in plant tissue to trigger visible HR and develops post-invasive defenses.

To summarize our findings on pear with a notion of cascading effect, we can propose the following scenario (Fig. 4): once *V. inaequalis* presence is recognized by pear, a calcium cellular influx is induced and leads to the development of a pre-invasive defense, the stomatal closure, but also promotes an early post-invasive defense, an apoplastic ROS accumulation. Apoplastic ROS, acting themselves as ubiquitous messengers, come to reinforce the stomatal closure but also mediate cellular signaling resulting in two post-invasive defenses: HR development at infection sites, along with phytoalexin (simple coumarin and hydroxicinnamic acid amines) production. The observed alterations of the epidermis composition (cellulose, pectin, lignin for the cell wall, and cutin for the cuticle), are presumed to strengthen this physical barrier and can be seen as the development of another pre-invasive defense. The calcium (action on pectin reviewed in [114]) and the ROS (action on lignin, [115]; [116]; action on cuticle, [117]) have been linked to some type of epidermis modifications and may participate in the proceeding of these defense in pear / *V. inaequalis* nonhost interaction.

Nonhost resistance is defined as the resistance of an entire plant species against a specific parasite or pathogen [118] and is seen as the most durable resistance of plant. Thus, understanding the molecular mechanisms underlying nonhost resistance can open up some interesting avenues to create sustainable host resistances in the same plant species. Considering pear, in order to stop the germination and entrance of hemibiotrophic host fungi such as *V. pyrina*, strengthening the cuticle initial barrier via more cutin production and cross-link, or promoting the biosynthesis of phytoalexins like hydroxycinnamic acid amines, appear as promising solutions, relatively easy to engineer regarding recent advances in biotechnology tools on this species ([119]; [120]; [121]).

Material and methods

Biological material

Apple plants from the cultivar 'Gala' and pear plants from the cultivar 'Conference' were chosen because of their susceptibility to *V. inaequalis* and *V. pyrina*, respectively. The apple and pear genotypes were multiplied in vitro, rooted and acclimatized in greenhouse as described previously ([122]; [123]).

For apple scab inoculation, the *V. inaequalis* monoconidial isolate used was EU-B05 from the European collection of *V. inaequalis* of the European project Durable Apple Resistance in Europe [124]. For pear scab inoculation, the monoconidial strain VP102 of *V. pyrina* was chosen for its aggressiveness on 'Conference' [125].

Scab inoculation procedure

Greenhouse growth conditions and mode of inoculum preparation were as described in Parisi and Lespinasse [126] for apple and Chevalier et al [127] for pear. Briefly, the youngest leaf of actively growing shoots was tagged and the plants inoculated with a conidial suspension (2×10^5 conidia ml^{-1}) of *Venturia pyrina* strain VP102 for apple and *Venturia inaequalis* strain EUB04 for pear. Symptoms

were recorded at 14, 21, 28, 35 and 42 days after inoculation. The type of symptoms was scored using the 6 class-scale of Chevalier et al [128].

Microscopic observations

Histological studies were made on samples stained with the fluorophore solophenylflavine [129]. In brief, leaf discs were rinsed in ethanol 50° before staining in a water solution of solophenylflavine 7GFE 500 (SIGMA-Aldrich, St Louis USA) 0.1% (v/v) for 10 min. The samples were first rinsed in deionized water, then in glycerol 25% for 10 min. Finally, the leaf samples were mounted on glass-slides in a few drops of glycerol 50%. They were examined with a wide-field epifluorescence microscope BH2-RFC Olympus (Hamburg, D) equipped with the following filter combination: excitation filter 395 nm and emission filter 504 nm.

Transcriptomics experiment

Leaf samples were immediately frozen in liquid nitrogen and kept at -80°C until analysis. Sampling concerned the youngest expanded leaf of each plant labeled the day of the inoculation. Each sample is a pool of leaves from three different plants and two biological repeats (n=2) have been made by condition (genotype x treatment x time). Leaf samples taken just before inoculation (T0) and at 24 and 72hpi, were then used to perform transcriptomics analyses.

For RNA extraction, frozen leaves were ground to a fine powder in a ball mill (MM301, Retsch, Hann, Germany). RNA was extracted with the kit NucleoSpin RNA Plant (Macherey Nagel, Düren, Germany) according to the manufacturer's instructions but with a modification: 4% of PVP40 (4 g for 100 ml) were mixed with the initial lysis buffer RAP before use. Purity and concentration of the samples were assayed with a Nanodrop spectrophotometer ND-1000 (ThermoFisher Scientific, Waltham, MA, USA) and by visualization on agarose gel (1% (weight/volume) agarose, TAE 0.5x, 3% (volume/volume) Midori green). Intron-spanning primers (forward primer: CTCTTGGTGTCAGGCAAATG, reverse primer: TCAAGGTTGGTGGACCTCTC) designed on the *EF-1α* gene (accession AJ223969 for apple and

PCP017051 for pear, available at https://www.rosaceae.org/, with the datasets on "Pyrus communis v1.0 draft genome") were used to check the absence of genomic DNA contamination by PCR. The PCR reaction conditions were as follows: 95°C for 5 min, followed by 35 cycles at 95°C for 30 s, 60°C for 45 s, 72°C for 1 min, with a final extension at 72°C for 5 min. The PCR products were separated on a 2% agarose gel.

Amplifications (aRNAs) were produced with MessageAmpII aRNA Kit (Ambion Invitrogen, Waltham, MA, USA), from 300 ng total RNA. Then 5 µg of each aRNA were retrotranscribed and labelled using a SuperScript II reverse transcriptase (Transcriptase inverse SuperScript™ II kit, Invitrogen, Carlsbad, CA, USA) and fluorescent dyes: either cyanine-3 (Cy3) or cyanine-5 (Cy5) (Interchim, Montluçon, France). Labeled samples (30 pmol each, one with Cy3, the other with Cy5) were combined two by two, depending on the experimental design. For each comparison two biological replicates were analyzed in dye-switch as described in Depuydt et al [130]. Paired labeled samples were then co-hybridized to Agilent microarray AryANE v2.0 (Agilent-070158_IRHS_AryANE-Venise, GPL26767 at GEO: https://www.ncbi.nlm.nih.gov/geo/) for apple, or Pyrus v1.0 (Agilent-078635_IRHS_Pyrus, GPL26768 at GEO) for pear, containing respectively 133584 (66792 sense and 66792 anti-sense probes) and 87812 (43906 sense and 43906 anti-sense probes) 60-mer oligonucleotide probes. The hybridizations were performed as described in Celton, Gaillard et al [131] using a MS 200 microarray scanner (NimbleGen Roche, Madison, WI, USA).

For microarray analysis we designed two new chips. For apple we used a deduplicated probeset from the AryANE v1.0 ([131]; 118740 probes with 59370 in sense and 59370 in anti-sense) augmented by 14844 probes (7422 in sense and 7422 in anti-sense) designed on new gene annotations from *Malus domestica* GDDH13 v1.1 (https://iris.angers.inra.fr/gddh13 or https://www.rosaceae.org/species/malus/malus_x_domestica/genome_GDDH13_v1.1). These probes target new coding genes with UTRs when available, manually curated micro-RNA precursors and transposable elements. For transposable elements we used one consensus sequence for each family and a randomly peaked number of elements proportionally to their respective abundance in

688 the genome. The microarray used in this study also have probes for coding genes of *V. inaequalis* but
689 they have not been taken into account.
690 For pear the design was done on the *Pyrus communis* Genome v1.0 Draft Assembly & Annotation
691 available on GDR (https://www.rosaceae.org/species/pyrus/pyrus_communis/genome_v1.0) web
692 site. We have downloaded the reference genome and gene predictions fasta files and structural
693 annotation gff file the 21st of September 2015. Using home-made Biopython scripts we have
694 extracted spliced CDS sequences with 60 nucleotides before start and after stop codons to get UTR-
695 like sequences likely to be found on transcripts resulting in a fasta file containing 44491 sequences.
696 These 60 nucleotides size increase the probability of finding specific probes on genes with high
697 similarity. This file was sent to the eArray Agilent probe design tool
698 (https://earray.chem.agilent.com/earray/) to generate one probe per gene prediction. Options used
699 were: Probe Length: 60, Probe per Target: 1, Probe Orientation: Sense, Design Options: Best Probe
700 Methodology, Design with 3' Bias. The probeset was then reverse-complemented to generate anti-
701 sense probes and filtered to remove duplicated probes. The final probeset contains 87812 unique
702 probes targeting 1 (73612 probes) or more (14200 probes) potential transcript both in sense and
703 anti-sense.
704 Normalization and statistical analyses performed to get normalized intensity values have been done
705 as in Celton, Gaillard et al [131]. For each comparison and each probe, we retrieved a ratio of the
706 logarithms of the fluorescence intensities (one per compared sample: T0 versus 24hpi or T0 versus
707 72hpi in our case) and an associated p-value. The applied p-value threshold to determine DEGs
708 (differentially expressed genes) was 0.05. Through blast analyze, a TAIR accession number (The
709 Arabidopsis Information Resource; https://www.arabidopsis.org/; [132]) has been linked to a
710 majority of apple or pear "probe/corresponding gene" and the couple "TAIR accession/ratio value"
711 has then been used to make a global analyze of functional categories observed in the Mapman
712 software (https://mapman.gabipd.org/homemapman.gabipd.org; [133]). The detailed analyze of
713 DEGs has been done through TAIR and KEGG (https://www.genome.jp/kegg/) databases, and

bibliography. Metadata for the 172 (162 for pear and 10 for apple) DEGs discussed in this work are available in Table S2 and S3 (Online only).

QPCR validation of transcriptomic data

In order to validate transcriptomic data, QPCR was performed on a selection of gene/sample associations. First-strand cDNA was synthesized using total RNA (2.0 µg) in a volume of 30 µl of 5× buffer, 0.5 µg of oligodT15 primer, 5 µl of dNTPs (2.5 mM each), and 150 units of MMLV RTase (Promega, Madison, WI, USA). The mixture was incubated at 42°C for 75 min. Quantitative RT-PCR (QPCR) was then performed. Briefly, 2.5 µl of the appropriately diluted samples were mixed with 5 µl of PerfeCTa SYBR Green SuperMix for iQ kit (Quantabio, Beverly, MA, USA) and 0.2 or 0.6 µl of each primer (10 µM) in a final volume of 10 µl. Primers were designed with Primer3Plus, their volumes were according to their optimal concentration (determined for reaction efficiency near to 100%; calculated as the slope of a standard dilution curve; [134]). Accessions, primer sequences and optimal concentrations are indicated in Table S1. The reaction was performed on a CFX Connect Real-Time System (BIO-RAD, Hercules, CA, USA) using the following program: 95°C, 5 min followed by 40 cycles comprising 95°C for 3 s, 60°C for 1 min. Melting curves were performed at the end of each run to check the absence of primer-dimers and nonspecific amplification products. Expression levels were calculated using the ΔΔCT method [135] and were corrected as recommended in Vandesompele et al [136], with three internal reference genes (GADPH, TUA and ACTIN 7 for apple, GADPH, TUA and EF1α for pear) used for the calculation of a normalization factor. For each couple DEG/sample (sample defining a plant, time, treatment and biological repeat combination), the ratio was obtained by dividing the mean value of CT calculated from 3 technical repeats by the normalization factor obtained for this sample.

Supplementary information

Additional File 1: Table S1, **S2** and **S3**.

Abbreviations

ABA: abscisic acid; CDPK: calcium dependent protein kinase; CRK: cysteine-rich receptor-like kinase; DEG: differentially expressed gene; DFR: dihydroflavonol 4-reductase; DGDG: digalactosyldiacylglycerol; ET: ethylene; ER: endoplasmic reticulum; ETI: effector triggered immunity; FAE: fatty acid elongase; GPAT: glycerol-3-phosphate acyltransferase; hpi: hours post inoculation; HR: hypersensitive reaction; JA; jasmonic acid; LCB: long chain/sphingoid base component; LCB-Ps: long chain base phosphate component; LOX: lipoxygenase; MAMP: microbe-associated molecular pattern; OPDA: 12-oxo-phytodienoic acid; PCD: programed cell death; PTI: pattern triggered immunity; RBOH: respiratory burst oxidase homolog; ROS: reactive oxygen species; SA: salicylic acid; SAR: systemic acquired resistance

Declarations

Acknowledgements

The authors gratefully acknowledge the IRHS-ImHorPhen team of INRA Angers for technical assistance in plant maintenance and the technical platforms ANAN and IMAC.

Authors contribution

EC, LP, and EV conceived the study. EC and EV supervised the study. ER and MB performed the biological experiments. SG and SP performed the database work and assisted with the bioinformatics analysis. EV wrote the original manuscript. EV and EC edited the manuscript. All authors have read and agreed to the published version of the manuscript.

Funding

This project was funded by the Synthé-Poir-Pom project (Angers University) and by the TIFON project (INRAE, department BAP).

Availability of data and materials

The datasets supporting the conclusion of this article are available in the Gene Expression Omnibus (GEO) repository [https://www.ncbi.nlm.nih.gov/geo/] with GSE159179 and GSE159180 accession numbers for apple and pear respectively.

Ethics approval and consent to participate

Experimental research on plants in this work comply with relevant institutional, national, and international guidelines and legislation.

Consent for publication

This section is not applicable.

Competing interests

The authors declare that they have no competing interests

References

1. Potter D, Eriksson T, Evans RC, Oh S, Smedmark JEE, Morgan DR, Kerr M, Robertson KR, et al. Phylogeny and classification of *Rosaceae*. Plant Syst Evol. 2007;266:5-43.
2. Campbell CS, Evans RC, Morgan DR, Dickinson TA, Arsenault MP. Phylogeny of subtribe *Pyrinae* (formerly the *Maloideae*, *Rosaceae*): Limited resolution of a complex evolutionary history. Plant Syst Evol. 2007;266: 119-145.
3. Wu J, Wang Z, Shi Z, Zhang S, Ming R, Zhu SL et al. The genome of pear (*Pyrus bretschneideri* Redh.). Genome Res. 2013;23:396-408.
4. Velasco R, Zharkikh A, Affourtit J, Dhingra A, Cestaro A, Kalyanaraman A et al. The genome of the domesticated apple (*Malus × domestica* Borkh.). Nature Genet. 2010;42:833–839.
5. Stehmann C, Pennycook S, Plummer K. Molecular identification of a sexual interloper: the pear pathogen *Venturia pirina*, has sex on apple. Phytopathol. 2001;91:663-541.

6. Rossman A, Castlebury L, Aguirre-Hudson B, Berndt R, Edwards. (2647–2651) Proposals to conserve the name *Venturia acerina* against *Cladosporium humile; Venturia borealis* against *Torulama culicola; Venturia carpophila* against *Fusicladium amygdali* and *Cladosporium americanum; Sphaerella inaequalis (Venturia inaequalis)* against *Spilocaea pomi, Fumago mali, Actinone macrataegi, Cladosporium dendriticum, Asteroma mali,* and *Scolicotrichum venosum;* and *Venturia pyrina* against *Helminthosporium pyrorum, Fusicladium virescens, F. fuscescens, Cladosporium polymorphum* and *Passalora pomi (Ascomycota: Dothideomycetes)*. Taxon. 2018;67:1209-1211.

7. Gonzalez-Dominguez E, Armengol J, Rossi V. Biology and epidemiology of *Venturia* species affecting fruit crops: a review. Front Plant Sci. 2017;8: 1496.

8. Jiang S, Park P, Ishii H. Penetration behaviour of *Venturia nashicola* , associated with hydrogen peroxide generation, in Asian and European pear leaves. J Phytopathol. 2014;162: 770-778.

9. Chevalier M, Bernard C, Tellier M, Audrain C, Durel CE. Host and non-host interactions of *Venturia inaequalis* and *Venturia pirina* on *Pyrus communis* and *Malus x domestica*. Acta Hortic. 2004;663: 205-208.

10. Lee HA, Lee HY, Seo E, Lee J, Kim SB, Oh S, Choi E, Choi E, Lee SE, Choi D. Current understanding of plant nonhost resistance. Mol Plant-Microbe Interact. 2017a;30:5-5.

11. Mysore JS, Ryu CM. Nonhost resistance: how much do we know? Trends Plant Sci. 2004;9: 97-104.

12. Perchepied L, Chevreau E, Ravon E, Gaillard S, Pelletier S, Bahut M, Berthelot P, Cournol R, Schouten HJ, Vergne E. Successful intergeneric transfer of a major apple scab resistance gene (Rvi6) from apple to pear and precise comparison of the downstream molecular mechanisms of this resistance in both species. bioRxiv 2021.05.31.446424; doi: https://doi.org/10.1101/2021.05.31.446424.

13. Wasternack C, Feussner I. The oxylipin pathways: biochemistry and function. Annu Rev Plant Biol. 2018;69:363-386.

814 14. Li C, Schilmiller AL, Liu G, Lee GI, Jayanty S, Sageman C, et al. Role of beta-oxidation in jasmonate
815 biosynthesis and systemic wound signaling in tomato. Plant Cell. 2005;17:971-986.
816 15. Seo JS, Koo YJ, Jung C, Yeu SY, Song JT, Kim JK, Choi Y, Lee JS, Do Choi Y. Identification of a novel
817 jasmonate-responsive element in the AtJMT promoter and its binding protein for AtJMT
818 repression. PLoS One. 2013;8:e55482.
819 16. Jeong JS, Jung C, Seo JS, Kim JK, Chua NH. The deubiquitinating enzymes UBP12 and UBP13
820 positively regulate MYC2 levels in jasmonate responses. Plant Cell. 2017;29:1406-1424.
821 17. Birkenbihl RP, Diezel C, Somssich IE. Arabidopsis WRKY33 is a key transcriptional regulator of
822 hormonal and metabolic responses toward *Botrytis cinerea* infection. Plant Physiol.
823 2012;159:266-85.
824 18. Kaurilind E, Xu E, Brosché M. A genetic framework for H2O2 induced cell death in *Arabidopsis*
825 *thaliana.* BMC Genomics. 2015;16:837.
826 19. Nurmberg PL, Knox KA, Yun BW, Morris PC, Shafiei R, Hudson A, Loake GJ. The developmental
827 selector AS1 is an evolutionarily conserved regulator of the plant immune response. Proc
828 Natl Acad Sci U.S.A. 2007;104:18795-187800.
829 20. Ali S, Ganai BA, Kamili AN, Bhat AA, Mir ZA, Bhat JA et al. Pathogenesis-related proteins and
830 peptides as promising tools for engineering plants with multiple stress tolerance. Microb Res.
831 2018; 212-213:29-37.
832 21. Li J, Brader G, Palva ET. The WRKY70 transcription factor: a node of convergence for jasmonate-
833 mediated and salicylate-mediated signals in plant defense. Plant Cell. 2004;16:319–331.
834 22. Li J, Brader G, Kariola T, Palva ET. WRKY70 modulates the selection of signaling pathways in plant
835 defense. Plant J. 2006;46:477–491.
836 23. Wang D, Amornsiripanitch N, Dong X. A genomic approach to identify regulatory nodes in the
837 transcriptional network of systemic acquired resistance in plants. PLoS Pathog. 2006;2:e123.
838 24. Li J, Zhong R, Palva ET. WRKY70 and its homolog WRKY54 negatively modulate the cell wall-
839 associated defenses to necrotrophic pathogens in Arabidopsis. PLoS One. 2017;12:e0183731.

840 25. Genot B, Lang J, Berriri S, Garmier M, Gilard F, Pateyron S, et al. Constitutively active Arabidopsis
841 MAP kinase 3 triggers defense responses involving salicylic acid and SUMM2 resistance
842 protein. Plant Physiol. 2017;174:1238-1249.
843 26. Hu X, Reddy AS. Cloning and expression of a PR5-like protein from Arabidopsis: inhibition of
844 fungal growth by bacterially expressed protein. Plant Mol Biol. 1997;34:949-59.
845 27. Mestre P, Arista G, Piron MC, Rustenholz C, Ritzenthaler C, Merdinoglu D, Chich JF. Identification
846 of a *Vitis vinifera* endo-β-1,3-glucanase with antimicrobial activity against *Plasmopara*
847 *viticola*. Mol Plant Pathol. 2017;18:708-719.
848 28. Zhang SB, Zhang WJ, Zhai HC, Lv YY, Cai JP, Jia F, Wang JS, Hu YS. Expression of a wheat β-1,3-
849 glucanase in Pichia pastoris and its inhibitory effect on fungi commonly associated with
850 wheat kernel. Protein Expres Purif. 2019;154:134-139.
851 29. Santamaria M, Thomson CJ, Read ND, Loake GJ; The promoter of a basic PR1-like gene, AtPRB1,
852 from Arabidopsis establishes an organ-specific expression pattern and responsiveness to
853 ethylene and methyl jasmonate. Plant Mol Biol. 2001;47:641-52.
854 30. Truman W, Sreekanta S, Lu Y, Bethke G, Tsuda K, Katagiri F, Glazebrook J. The CALMODULIN-
855 BINDING PROTEIN60 family includes both negative and positive regulators of plant immunity.
856 Plant Physiol. 2013;163:1741-1751.
857 31. Boursiac Y, Lee SM, Romanowsky S, Blank R, Sladek C, Chung WS, Harper JF. Disruption of the
858 vacuolar calcium-ATPases in Arabidopsis results in the activation of a salicylic acid-dependent
859 programmed cell death pathway. Plant Physiol. 2010;154:1158-71.
860 32. Huang J, Sun Y, Orduna AR, Jetter R, Li X. The Mediator kinase module serves as a positive
861 regulator of salicylic acid accumulation and systemic acquired resistance. Plant J. 2019;98:842-
862 852.
863 33. Wang W, Tang W, Ma T, Niu D, Jin JB, Wang H, Lin R. A pair of light signaling factors FHY3 and
864 FAR1 regulates plant immunity by modulating chlorophyll biosynthesis. Journal of Integrative
865 Plant Biol. 2015;58:91-103.

866 34. Song JT, Koo YJ, Seo HS, Kim MC, Choi YD, Kim JH. Overexpression of AtSGT1, an Arabidopsis
867 salicylic acid glucosyltransferase, leads to increased susceptibility to *Pseudomonas syringae*.
868 Phytochemistry. 2008;69:1128-34.
869 35. Vlot AC, Dempsey DA, Klessig DF. Salicylic acid, a multifaceted hormone to combat disease. Annu
870 Rev Phytopathol. 2009;47:177-206.
871 36. Andreasson E, Jenkins T, Brodersen P, Thorgrimsen S, Petersen NH, Zhu S et al. The MAP kinase
872 substrate MKS1 is a regulator of plant defense responses. EMBO J. 2005;24:2579-89.
873 37. Xia Y, Yu K, Gao QM, Wilson EV, Navarre D, Kachroo P, Kachroo A. Acyl CoA binding proteins are
874 required for cuticle formation and plant responses to microbes. Front Plant Sci. 2012;3:224.
875 38. Boller T, Felix G. A renaissance of elicitors: perception of microbe-associated molecular patterns
876 and danger signals by pattern recognition receptors. Annu Rev Plant Biol. 2009;60:379-406.
877 39. Vincill ED, Bieck AM, Spalding EP. Ca(2+) conduction by an amino acid-gated ion channel related
878 to glutamate receptors. Plant Physiol. 2012;159:40-46.
879 40. Hou C, Tian W, Kleist T, He K, Garcia V, Bai F, Hao Y, Luan S, Li L. DUF221 proteins are a family of
880 osmosensitive calcium-permeable cation channels conserved across eukaryotes. Cell Res.
881 2014;24:632-635.
882 41. Fonseca JP, Mysore KS. Genes involved in nonhost disease resistance as a key to engineer durable
883 resistance in crops. Plant Sci. 2019;279:108-116.
884 42. Ronzier E, Corratgé-Faillie C, Sanchez F, Prado K, Brière C, Leonhardt N, Thibaud JB, Xiong TC.
885 CPK13, a noncanonical Ca2+-dependent protein kinase, specifically inhibits KAT2 and KAT1
886 shaker K+ channels and reduces stomatal opening. Plant Physiol. 2014;166:314-26.
887 43. Zou JJ, Li XD, Ratnasekera D, Wang C, Liu WX, Song LF, Zhang WZ, Wu WH. Arabidopsis CALCIUM-
888 DEPENDENT PROTEIN KINASE8 and CATALASE3 function in abscisic acid-mediated signaling
889 and H2O2 homeostasis in stomatal guard cells under drought stress. Plant Cell.
890 2015;27:1445-1460.

891 44. Förster S, Schmidt LK, Kopic E, Anschütz U, Huang S, Schlücking K, et al. Wounding-induced
892 stomatal closure requires jasmonate-mediated activation of GORK K(+) channels by a Ca(2+)
893 sensor-kinase CBL1-CIPK5 complex. Dev Cell. 2019;48:87-99.e6.
894 45. Kadota Y, Shirasu K, Zipfel C. Regulation of the NADPH oxidase RBOHD during plant immunity.
895 Plant Cell Physiol. 2015;56: 1472–1480.
896 46. Adachi H, Yoshioka H. Kinase-mediated orchestration of NADPH oxidase in plant immunity. Brief
897 Funct Genomics. 2015;14:253-259.
898 47. Zhai L, Sun C, Feng Y, Li D, Chai X, Wang L, Sun Q, et al. AtROP6 is involved in reactive oxygen
899 species signaling in response to iron-deficiency stress in Arabidopsis thaliana. FEBS Lett.
900 2018;592:3446-3459.
901 48. Gao X, Chen X, Lin W, Chen S, Lu D, Niu Y, Li L, Cheng C, McCormack M, Sheen J, Shan L, He P.
902 Bifurcation of Arabidopsis NLR immune signaling via Ca^{2+}-dependent protein kinases. PLoS
903 Pathog. 2013;9:e1003127.
904 49. Qi J, Wang J, Gong Z, Zhou JM. Apoplastic ROS signaling in plant immunity. Curr Opin Plant Biol.
905 2017;38:92-100.
906 50. Bourdais G, Burdiak P, Gauthier A, Nitsch L, Salojärvi J, Rayapuram C et al. CRK consortium large-
907 scale phenomics identifies primary and fine-tuning roles for CRKs in responses related to
908 oxidative stress. PLoS Genet. 2015;11:e1005373.
909 51. Sun T, Nitta Y, Zhang Q, Wu D, Tian H, Lee JS, Zhang Y. Antagonistic interactions between two
910 MAP kinase cascades in plant development and immune signaling. EMBO Rep.
911 2018;19:e45324.
912 52. O'Brien JA, Daudi A, Butt VS, Bolwell GP. Reactive oxygen species and their role in plant defence
913 and cell wall metabolism. Planta. 2012;236:765-779.
914 53. Brosché M, Blomster T, Salojärvi J, Cui F, Sipari N, Leppälä J et al. Transcriptomics and functional
915 genomics of ROS-induced cell death regulation by RADICAL-INDUCED CELL DEATH1. PLoS
916 Genet. 2014;10:e1004112.

54. Cheng YT, Li Y, Huang S, Huang Y, Dong X, Zhang Y, Li X. Stability of plant immune-receptor resistance proteins is controlled by SKP1-CULLIN1-F-box (SCF)-mediated protein degradation. Proc Natl Acad Sci U.S.A. 2011;108:14694-14699.

55. Coll NS, Vercammen D, Smidler A, Clover C, Van Breusegem F, Dangl JL, Epple P. Arabidopsis type I metacaspases control cell death. Science. 2010;330:1393-1397.

56. Lema-Asqui S, Vercammen D, Serrano I, Valls M, Rivas S, Van Breusegem F, et al. AtSERPIN1 is an inhibitor of the metacaspase AtMC1-mediated cell death and autocatalytic processing in planta. New Phytol. 2018;218:1156-1166.

57. Kawasaki T, Nam J, Boyes DC, Holt BF, Hubert DA, Wiig A, Dangl JL. A duplicated pair of Arabidopsis RING-finger E3 ligases contribute to the RPM1-and RPS2-mediated hypersensitive response. Plant J. 2005;44: 258-270.

58. Luo H, Laluk K, Lai Z, Veronese P, Song F, Mengiste T. The Arabidopsis Botrytis Susceptible1 interactor defines a subclass of RING E3 ligases that regulate pathogen and stress responses. Plant Physiol. 2010;154:1766-1782.

59. Huby E, Napier JA, Baillieul F, Michaelson LV, Dhondt-Cordelier S. Sphingolipids: towards an integrated view of metabolism during the plant stress response. New Phytol. 2020;225:659-670.

60. Saucedo-Garcia M, Guevara-Garcia A, Gonzalez-Solis A, Cruz-Garcia F, VazquezSantana S, Markham JE, et al. MPK6, sphinganine and the LCB2a gene from serine palmitoyltransferase are required in the signaling pathway that mediates cell death induced by long chain bases in Arabidopsis. New Phytol. 2011;191:943–957.

61. Veley KM, Maksaev G, Frick EM, January E, Kloepper SC, Haswell ES. Arabidopsis MSL10 has a regulated cell death signaling activity that is separable from its mechanosensitive ion channel activity. Plant Cell. 2014;26:3115-3131.

62. Guerringue Y, Thomine S, Frachisse JM. Sensing and transducing forces in plants with MSL10 and DEK1 mechanosensors. FEBS Lett. 2018;592:1968-1979.

943 63. Zhao C, Nie H, Shen Q, Zhang S, Lukowitz W, Tang D. EDR1 physically interacts with MKK4/MKK5
944 and negatively regulates a MAP kinase cascade to modulate plant innate immunity. PLoS
945 Genet. 2014;10:e1004389.
946 64. Lee MH, Jeon HS, Kim HG, Park OK. An Arabidopsis NAC transcription factor NAC4 promotes
947 pathogen-induced cell death under negative regulation by microRNA164. New Phytol.
948 2017b;214:343-360.
949 65. Najafi J, Brembu T, Vie AK, Viste R, Winge P, Somssich IE, Bones AM. PAMP-INDUCED SECRETED
950 PEPTIDE 3 modulates immunity in Arabidopsis. J Exp Bot. 2020;71:850-864.
951 66. Khafif M, Balagué C, Huard-Chauveau C, Roby D. An essential role for the VASt domain of the
952 Arabidopsis VAD1 protein in the regulation of defense and cell death in response to
953 pathogens. PLoS One. 2017;12:e0179782.
954 67. Mittler R, Herr EH, Orvar BL, van Camp W, Willekens H, Inzé D, Ellis BE. Transgenic tobacco plants
955 with reduced capability to detoxify reactive oxygen intermediates are hyperresponsive to
956 pathogen infection. Proc Natl Acad Sci U.S.A. 1999;96:14165-70.
957 68. Simon C, Langlois-Meurinne M, Didierlaurent L, Chaouch S, Bellvert F, Massoud K, et al. The
958 secondary metabolism glycosyltransferases UGT73B3 and UGT73B5 are components of redox
959 status in resistance of Arabidopsis to *Pseudomonas syringae* pv. *tomato*. Plant Cell Environ.
960 2014;37:1114-1129.
961 69. Bacete L, Mélida H, Miedes E, Molina A. Plant cell wall-mediated immunity: cell wall changes
962 trigger disease resistance responses. Plant J. 2018;93:614-636.
963 70. Miedes E, Vanholme R, Boerjan W, Molina A. The role of the secondary cell wall in plant
964 resistance to pathogens. Front Plant Sci. 2014;5:358.
965 71. Fich EA, Segerson NA, Rose JK. The plant polyester cutin: biosynthesis, structure, and biological
966 roles. Ann Rev Plant Biol. 2016;67:207-233.
967 72. Lim GH, Singhal R, Kachroo A, Kachroo P. Fatty acid- and lipid-mediated signaling in plant defense.
968 Annu Rev Phytopathol. 2017;55:505-536.

969 73. Joubès J, Raffaele S, Bourdenx B, Garcia C, Laroche-Traineau J, Moreau P, Domergue F, Lessire R.
970 The VLCFA elongase gene family in *Arabidopsis thaliana*: phylogenetic analysis, 3D modelling
971 and expression profiling. Plant Mol Biol. 2008;67:547-66.
972 74. Lee SB and Suh MC. Advances in the understanding of cuticular waxes in *Arabidopsis thaliana* and
973 crop species. Plant Cell Rep. 2015;34:557-572.
974 75. Li Y, Beisson F, Koo AJ, Molina I, Pollard M, Ohlrogge J. Identification of acyltransferases required
975 for cutin biosynthesis and production of cutin with suberin-like monomers. Proc Natl Acad Sci
976 U.S.A. 2007;104:18339-18344.
977 76. Yeats TH, Huang W, Chatterjee S, Viart HM, Clausen MH, Stark RE, Rose JK. Tomato Cutin
978 Deficient 1 (CD1) and putative orthologs comprise an ancient family of cutin synthase-like
979 (CUS) proteins that are conserved among land plants. Plant J. 2014;77:667-675.
980 77. Cui F, Brosche M, Lehtonen MT, Amiryousefi A, Xu E, Punkkinen M, Valkonen JPT, Fujii H,
981 Overmyer K. Dissecting abscisic acid signaling pathways involved in cuticle formation. Mol
982 Plant. 2016;9: 926-938.
983 78. Yang L, Wen KS, Ruan X, Zhao YX, Wei F, Wang Q**.** Response of plant secondary metabolites to
984 environmental factors. Molecules. 2018;23i:e762.
985 79. Tetali S. Terpenes and isoprenoids: a wealth of compounds for global use. Planta. 2019;249:1-8.
986 80. Wang K, Senthil-Kumar M, Ryu CM, Kang L, Mysore KS. Phytosterols play a key role in plant innate
987 immunity against bacterial pathogens by regulating nutrient efflux into the apoplast. Plant
988 Physiol. 2012;158:1789-1802.
989 81. Falcone Ferreyra ML, Emiliani J, Rodriguez EJ, Campos-Bermudez VA, Grotewold E, Casati P. The
990 identification of maize and Arabidopsis type I FLAVONE SYNTHASEs links flavones with
991 hormones and biotic interactions. Plant Physiol. 2015;169:1090-107.
992 82. Wang N, Xu H, Jiang S, Zhang Z, Lu N, Qiu H, Qu C, Wang Y, Wu S, Chen X. MYB12 and MYB22 play
993 essential roles in proanthocyanidin and flavonol synthesis in red-fleshed apple (*Malus*
994 *sieversii* f. *niedzwetzkyana*). Plant J. 2017a;90:276-292.

995 83. Zhai R, Zhao Y, Wu M, Yang J, Li X, Liu H, Wu T, Liang F, Yang C, Wang Z, Ma F, Xu L. The MYB
996 transcription factor PbMYB12b positively regulates flavonol biosynthesis in pear fruit. BMC
997 Plant Biol. 2019;19:85.
998 84. Wang XC, Wu J, Guan ML, Zhao CH, Geng P, Zhao Q. Arabidopsis MYB4 plays dual roles in
999 flavonoid biosynthesis. Plant J. 2020;101:637-652.
1000 85. Fernández-Pérez F, Vivar T, Pomar F, Pedreño MA, Novo-Uzal E. Peroxidase 4 is involved in
1001 syringyl lignin formation in *Arabidopsis thaliana*. J Plant Physiol. 2015a;175:86-94.
1002 86. Zhao Q, Nakashima J, Chen F, Yin Y, Fu C, Yun J, Shao H, Wang X, Wang ZY, Dixon RA. Laccase is
1003 necessary and nonredundant with peroxidase for lignin polymerization during vascular
1004 development in Arabidopsis. Plant Cell. 2013;25:3976-3987.
1005 87. Cosio C, Ranocha P, Francoz E, Burlat V, Zheng Y, Perry SE, Ripoll JJ, Yanofsky M, Dunand C. The
1006 class III peroxidase PRX17 is a direct target of the MADS-box transcription factor AGAMOUS-
1007 LIKE15 (AGL15) and participates in lignified tissue formation. New Phytol. 2017;213:250-263.
1008 88. Tokunaga N, Kaneta T, Sato S, Sato Y. Analysis of expression profiles of three peroxidase genes
1009 associated with lignification in Arabidopsis thaliana. Physiol Plantarum. 2009;136:237-249.
1010 89. Fernández-Pérez F, Pomar F, Pedreño MA, Novo-Uzal E. The suppression of AtPrx52 affects fibers
1011 but not xylem lignification in Arabidopsis by altering the proportion of syringyl units. Physiol
1012 Plantarum. 2015b;154:395-406.
1013 90. Vilanova L, Teixidó N, Torres R, Usall J, Viñas I. The infection capacity of *P. expansum* and *P.*
1014 *digitatum* on apples and histochemical analysis of host response. International Journal of
1015 Food Microbiol. 2012;157:360-367.
1016 91. Fink W, Haug M, Deising H, Mendgen K. Early defence responses of cowpea *(Vigna sinensis* L.)
1017 induced by non-pathogenic rust fungi. Planta. 1991;185:246-254.
1018 92. Song PP, Zhao J, Liu ZL, Duan YB, Hou YP, Zhao CQ, Wu M, Wei M, Wang NH, Lv Y, Han ZJ.
1019 Evaluation of antifungal activities and structure-activity relationships of coumarin derivatives.
1020 Pest Manag. Sci. 2017;73:94-101.

93. Giesemann A, Biehl B, Lieberei R. Identification of scopoletin as a phytoalexin of the rubber tree *Hevea brasiliensis*. J Phytopathol. 1986;117:373–376.

94. Muroi A, Ishihara A, Tanaka C, Ishizuka A, Takabayashi J, Miyoshi H, Nishioka T. Accumulation of hydroxycinnamic acid amides induced by pathogen infection and identification of agmatine coumaroyltransferase in *Arabidopsis thaliana*. Planta. 2009;230:517-527.

95. Dobritzsch M, Lübken T, Eschen-Lippold L, Gorzolka K, Blum E, Matern A et al. MATE transporter-dependent export of hydroxycinnamic acid amides. Plant Cell. 2016;28:583-96.

96. Celoy RM, VanEtten HD. (+)-Pisatin biosynthesis: from (-) enantiomeric intermediates via an achiral 7,2'-dihydroxy-4',5'-methylenedioxyisoflav-3-ene. Phytochem. 2014;98:120-127.

97. Vorwieger A, Gryczka C, Czihal A, Douchkov D, Tiedemann J, Mock HP, et al. Iron assimilation and transcription factor controlled synthesis of riboflavin in plants. Planta. 2007;226:147-158.

98. Trapalis M, Li SF, Parish RW. The Arabidopsis GASA10 gene encodes a cell wall protein strongly expressed in developing anthers and seeds. Plant Sci. 2017;260:71-79.

99. Yamauchi Y, Hasegawa A, Mizutani M, Sugimoto Y. Chloroplastic NADPH-dependent alkenal/one oxidoreductase contributes to the detoxification of reactive carbonyls produced under oxidative stress. FEBS Lett. 2012;586:1208-1213.

100. Segond D, Dellagi A, Lanquar V, Rigault M, Patrit O, Thomine S, Expert D. NRAMP genes function in *Arabidopsis thaliana* resistance to *Erwinia chrysanthemi* infection. Plant J. 2009;58:195-207.

101. Lee MW, Jelenska J, Greenberg JT. Arabidopsis proteins important for modulating defense responses to *Pseudomonas syringae* that secrete HopW1-1. Plant J. 2008;54:452-445.

102. Hong GJ, Xue XY, Mao YB, Wang LJ, Chen XY. Arabidopsis MYC2 interacts with DELLA proteins in regulating sesquiterpene synthase gene expression. Plant Cell. 2012;24:2635-2648.

103. Rodriguez-Saona CR, Polashock J, Malo EA. Jasmonate-mediated induced volatiles in the American cranberry, *Vaccinium macrocarpon*: from gene expression to organismal interactions. Front Plant Sci. 2013;4:115.

104. Simanshu DK, Zhai X, Munch D, Hofius D, Markham JE, Bielawski J, et al. Arabidopsis accelerated cell death 11, ACD11, is a ceramide-1-phosphate transfer protein and intermediary regulator of phytoceramide levels. Cell Rep. 2014;6:388-399.

105. Fink L, Kwapiszewska G, Wilhelm J, Bohle RM. Laser-microdissection for cell type- and compartment-specific analyses on genomic and proteomic level. Exp Toxicol Pathol. 2006;57 Suppl 2:25-259.

106. Yan Y, Zheng XF, Apaliya MT, Yang HJ, Zhang HY. Transcriptome characterization and expression profile of defense-related genes in pear induced by *Meyerozyma guilliermondii*. Postharvest Biol Technol. 2018;141:63-70.

107. Zhang Q, Zhao L, Li B, Gu X, Zhang X, Boateng NS, Zhang H. Molecular dissection of defense response of pears induced by the biocontrol yeast, *Wicherhamomyces anomalus* using transcriptomics and proteomics approaches. Biol Control. 2020;148:104305.

108. Wang H, lin J, Chang YH, Jiang CZ. Comparative transcriptomic analysis reveals that ethylene/H2O2-mediated hypersensitive response and programmed cell death determine the compatible interaction of sans pear and *Alternaria alternate.* Front Plant Sci. 2017b;8:196.

109. Xu M, Yang Q, Boateng NAS, Ahima J, Dou Y, Zhang H. Ultrastructure observation and transcriptome analysis of *Penicillium expansum* invasion in postharvest pears. Postharvest Biol Technol. 2020;165:111198.

110. Gill US, Lee S, Mysore KS. Host versus nonhost resistance: distinct wars with similar arsenals. Phytopathol. 2015;105:580-587.

111. Pieterse CM, Van der Does D, Zamioudis C, Leon-Reyes A, Van Wees SC. Hormonal modulation of plant immunity. Annu Rev Cell Dev Biol. 2012;28:489-521.

112. Tsuda K, Sato M, Stoddard T, Glazebrook J, Katagiri F. Network properties of robust immunity in plants. PLoS Genet. 2009;5(12):e1000772.

113. Velho AC, Stadnik MJ. Non-host resistance of arabidopsis and apple is associated with callose accumulation and changes in preinfective structures of *Colletotrichum* species. Physiol Mol Plant Pathol. 2020;110:101463.

114. Thor K. Calcium-nutrient and messenger. Front Plant Sci. 2019 ;10:440.

115. Das K and Roychoudhury A. Reactive oxygen species (ROS) and response of antioxidants as ROS-scavengers during environmental stress in plants. Front Envir Sci. 2014;2:53.

116. Lehmann S, Serrano M, L'Haridon F, Tjamos SE, Metraux JP. Reactive oxygen species and plant resistance to fungal pathogens. Phytochemistry. 2015;112:54-62.

117. Survila M, Davidsson PR, Pennanen V, Kariola T, Broberg M, Sipari N, Heino P, Palva ET. Peroxidase-generated apoplastic ROS impair cuticle integrity and contribute to DAMP-elicited defenses. Front Plant Sci. 2016; 7:1945.

118. Heath MC. Nonhost resistance and nonspecific plant defenses. Curr Opin Plant Biol. 2000;3:315-319.

119. Charrier A, Vergne E, Dousset N, Richer A, Petiteau A, Chevreau E. Efficient targeted mutagenesis in apple and first time edition of pear using the CRISPR/Cas9 system. Front Plant Sci. 2019;10:40.

120. Chevreau E, Evans K, Montanari S Chagné D. Ch.19.9 Pyrus spp. Pear and Cydonia spp. Quince. In: Litz RE, Pliego-Alfaro F, Hormaza JL, editors. Biotechnology of Fruit and Nut Crops, 2nd edition. C.A.B. International, Wallingford, UK; 2020;p. 581-605.

121. Malabarba J, Chevreau E, Dousset N, Veillet F, Moizan J, Vergne E. New strategies to overcome present CRISPR/Cas9 limitations in apple and pear: efficient dechimerization and base editing. Int J Mol Sci. 2020;22:319.

122. Faize M, Malnoy M, Dupuis F, Chevalier M, Parisi L, Chevreau E. Chitinases of *Trichoderma atroviridae* induce scab resistance and some metabolic changes in two cultivars of apple. Phytopathol. 2003;93:1496-1504.

123. Leblay C, Chevreau E, Raboin LM. Adventitious shoot regeneration from in vitro leaves of several pear cultivars (*Pyrus communis* L.). Plant Cell Tissue Organ Cult. 1991;25:99-105.

124. Lespinasse Y, Durel CE, Parisi L, Laurens F, Chevalier M, Pinet C. A European project: D.A.R.E. Durable apple resistance in Europe. Acta Hortic. 2000;538:197–200.

125. Chevalier M, Tellier M, Lespinasse Y, Bruynincks M, Georgeault S. Behaviour studies of new races of *Venturia pirina* isolated from 'Conference' cultivar on a range of pear cultivars. Acta Hortic. 2008a;800:817-824.

126. Parisi L, Lespinasse Y. Pathogenicity of *Venturia inaequalis* strains of race 6 on apple clone (*Malus sp*.). Plant Dis. 1996;80: 1179-1183.

127. Chevalier M, Tellier M, Lespinasse Y, Caffier V. How to optimize the *Venturia* pirina inoculation on pear leaves in greenhouse conditions? Acta Hortic. 2008b;800: 913-920.

128. Chevalier M, Lespinasse Y, Renaudin S. A microscopic study of different classes of symptoms coded by the *Vf* gene in apple resistance to scab (*Venturia inaequalis*). Plant Pathol. 1991;40: 249–256.

129. Hoch HC, Galvani CD, Szarowski DH, Turner JN. Two new fluorescent dyes applicable for visualization of fungal cell walls. Mycologia. 2005;97: 580-588.

130. Depuydt S, Trenkamp S, Fernie AR, Elftieh S, Renou J-P, Vuylsteke M, Holster M, Vereecke D. An integrated genomic approach to define niche establishment by *Rhodococcus fascians* . Plant Physiol. 2009;149: 1366–1386.

131. Celton JM, Gaillard S, Bruneau M, Pelletier S, Aubourg S, Martin-Magniette ML, Navarro L, Laurens F, Renou JP. Widespread anti-sense transcription in apple is correlated with siRNA production and indicates a large potential for transcriptional and/or post-transcriptional control. New Phytol. 2014;203:287-99.

132. Berardini TZ, Reiser L, Li D, Mezheritsky Y, Muller R, Strait E, Huala E. The Arabidopsis information resource: Making and mining the "gold standard" annotated reference plant genome. Genesis. 2015;53:474-85.

133. Thimm O, Bläsing O, Gibon Y, Nagel A, Meyer S, Krüger P, Selbig J, Müller LA, Rhee SY, Stitt M. MAPMAN: a user-driven tool to display genomics data sets onto diagrams of metabolic pathways and other biological processes. Plant J. 2004;37:914-939.

134. Pfaffl MW. A new mathematical model for relative quantification in real-time RT-PCR. Nucleic Acids Res. 2001;29, e45.

135. Livak KJ, Schmittgen TD. Analysis of relative gene expression data using real-time quantitative PCR and the 2−ΔΔCT method. Methods. 2001;25:402-408.

136. Vandesompele, J., De Preter, K., Pattyn, F., Poppe, B., Van Roy, N., De Paepe, A. et al. Accurate normalization of real-time quantitative RT-PCR data by geometric averaging of multiple internal control genes. Genome Biol. 2002;3(7):00341-003411.

Figure legends

Fig. 1: **Macro- and microscopic observations of nonhost interactions.**

Binocular observation 21 days after *V. inaequalis* inoculation on 'Conference' (A) and (B) and *V. pyrina* inoculation on 'Gala' (C). Wide field fluorescence observations of: 'Conference' 3 days (D) and 14 days (E) after *V. inaequalis* inoculation, 'Gala' 3 days (F) and 14 days (G) after *V. pyrina* inoculation. Ap: appressorium, C: conidia, Gf: germination filament, Pp: pin point

Fig. 2: **Functional categories of DEGs at 24 or 72hpi during pear response to *V. inaequalis*.**

The number of up- or down-regulated DEGs is expressed as a percentage of the total number of genes present in the Pyrus v1.0 (87812 probes) microarray. DEGs are classified in functional categories according to MapMan 3.5.1R2 bins. Only bins with ≥ 6 DEGs are presented.

Fig. 3: DEGs involved in hormonal pathways during pear/*V. inaequalis* non-host interaction.

A: DEGs involved in JA pathway; B: DEGs involved in SA pathway. Genes written in red are induced, genes written in blue are repressed. ACA11: autoinhibited $Ca2^{+}$-ATPase, calmodulin-activated $Ca2^{+}$ pumps at the plasma membrane, endoplasmic reticulum, and vacuole. ACBP6: acyl-CoA-binding protein. ACX4: acyl-CoA-oxidase1. AS1/MYB91: Asymmetric leaves 1 transcription factor, CAMTA1: calmodulin-binding transcription activator, CBP60a: calmodulin-binding protein 60a, EDS1: enhanced disease suceptibility 1. FAR1: FAR-red impaired response 1. G-box: cis-element in the promoter. JAZ: jasmonate-zim domain protein, JMT: jasmonic acid carboxyl methyltransferase. LOX: lipoxygenase, MES1: methylesterase 1. MFP2: multifunctional protein 2. MKS1: MAP kinase substrate 1. MYC2: transcription factor. NINJA: novel interactor of JAZ. PAD4: phytoalexin deficient 4. UGT74F1: glucosyltransferase. PR1-like (with ATPRB1), PR2, PR3, PR4 (HEL and ATEP3), PR5, PR12: pathogenesis-related proteins. ST2A: sulfotransferase 2A. TPL: TOPLESS co-repressor. UBP12: ubiquitin-specific protease 12. WRKY: transcription factor.

Fig. 4: **Scenario of major events observed while three first days of pear/*V. inaequalis* non-host interaction.**

On the left side, events observed in a typical cell, on the right side, events observed in guard cells of a stomata. A: apoplasm, AP: appressorium, C: cuticle, CBL1: calcineurin B-like protein 1, CDPK: Ca_2^{+}-dependent protein kinases, CRK: cysteine-rich receptor-like kinase, CY: cytoplasm, CW: cell wall, HAA: hydroxycinnamic acid amines, HR: hypersensitive response, JA: jasmonic acid, MB: plasma membrane, LCB: Long Chain/sphingoid Base components, MPK6: Mitogen activated protein kinase 6, MSL10: mechano-sensitive like 10, N: nucleus, PH: penetration hypha, PR: pathogenesis related proteins, RBOHB: respiratory burst oxidase homolog B, ROS: reactive oxygen species, S: stomata, SA: salycilic acid, SC: simple coumarins, SP: spore.

Fig. 5: Main DEGs involved in cutin and wax biosynthesis during pear/V. inaequalis non-host interaction.

In green the chloroplast, in brown the endoplastic reticulum (ER) and in yellow the nucleus. Genes written in red are induced, genes written in blue are repressed. FAS: Fatty Acid Synthase complex to which belong ACCD (carboxytransferase beta subunit of the Acetyl-CoA carboxylase complex), FabG (β-ketoacyl ACP-reductase) and MOD1 (enoyl-ACP-reductase) functions. FAE: fatty acid elongase complex. KCS4 (3-ketoacyl-CoA synthase 4) and ECR/CER10 (trans-2-enoyl-CoA reductase) belong to the FAE complex. CER1 (octadecanal decarbonylase) and CER3 are implicated in aldehydes (CER1) and alkanes (CER1 and 3) generation in waxes biosynthesis. In cutin monomers synthesis, the ω-hydroxylation of C16:0 and C18:1 is catalyzed by cytochrome P450 monooxygenase (CYP86A) and LACS-encoded acyl-CoA synthetase may be required either to synthesize 16-hydroxy 16:0-CoA, a substrate for ω-hydroxylase, or for membrane transfer of monomers. Finally, the mature monoacylglycerol cutin monomers are generated by transfer of the acyl group from acyl-CoA to glycerol-3-phosphate by glycerol-3-phosphate acyltransferase (GPAT) enzymes such as GPAT8. Some GDSL-lipases enzyme (such as At1g28600, At1g28660, At1g54790, At3g16370, At3g48460, AtCUS4: At4g28780, At5g14450) are then functioning as cutin synthase and polymerize cutin monoacylglycerols. Transcription factors such as MYB16 and SHN1 are positive regulators of wax and cutin biosynthesis. Adapted from Xia et al, 2009, [71] and [72].

Fig. 6: Main DEGs involved in the phenylpropanoid pathway during Pear / *V. inaequalis* non-host interaction.

Genes framed in red are induced, genes frames in blue are repressed. Framed in black, the detail of genes involved in flavonoids production and found in this interaction. Abbreviations: 4CL, 4-coumarate-CoA ligase; AACT, anthocyanin 5-aromatic acyltransferase; ANR, anthocyanidin reductase; ANS, anthocyanin synthase; BGLC or BGLU, β-glucosidases; C3H, coumarate 3-hydroxylase; C4H, cinnamate 4-hydroxylase; CAD, cinnamyl alcohol dehydrogenase; CCoAOMT, caffeoyl-CoA O-methyltransferase; CCR, cinnamoyl-CoA reductase; CHI, chalcone isomerase; CHS, chalcone synthase; COMT, caffeic acid 3-O-methyltransferase; CPK, calcium-dependent protein kinase ; DFR,

dihydroflavonol reductase; DMR6, downy mildiou resistant 6; F3H, flavanone 3-hydroxylase; F3'H flavonoid 3'-hydroxylase; FLS, flavonol synthase; FNS, flavone synthase; GGT1, gamma-glutamyl transpeptidase 1; GT, glucosyl transferase; HCT, hydroxycinnamoyl-CoA shikimate/quinate hydroxycinnamoyl transferase; LAC, laccase; LAR, leucoanthocyanidin reductase; OMT1, O-methyltransferase 1; PAL, phenylalanine ammonia-lyase; PER or PRX, peroxidase; TT7, transparent testa 7; UGFT, UDP-glucose flavonoid-3-O-glucosyltransferase; UGT71D1, UDP-glycosyltransferase 71D1.

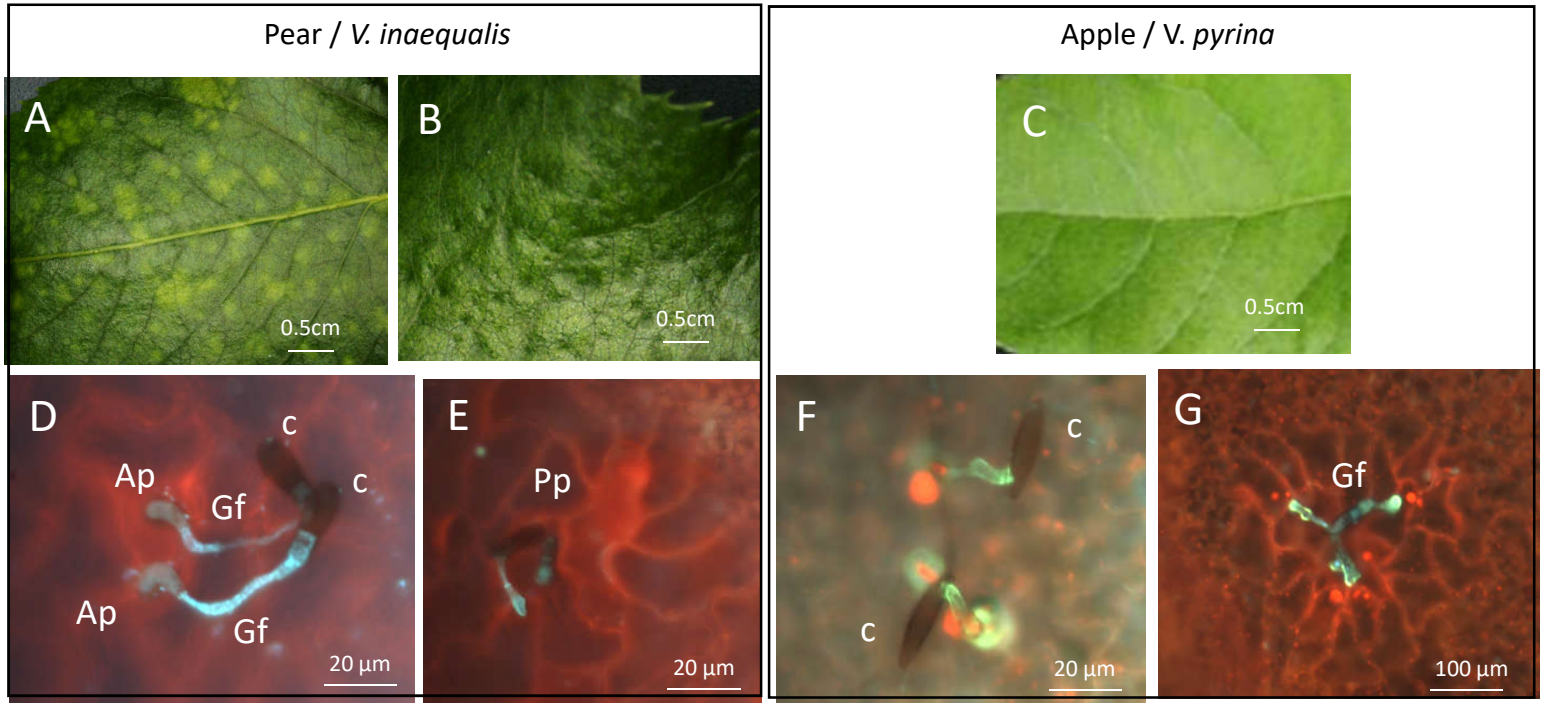
Pear / V. inaequalis
Apple / V. pyrina
A
0.5cm
B
0.5cm
C
0.5cm
D
c
Ap
Gf
c
Ap
Gf
20 µm
E
Pp
20 µm
F
c
c
20 µm
G
Gf
100 µm

Fig. 1

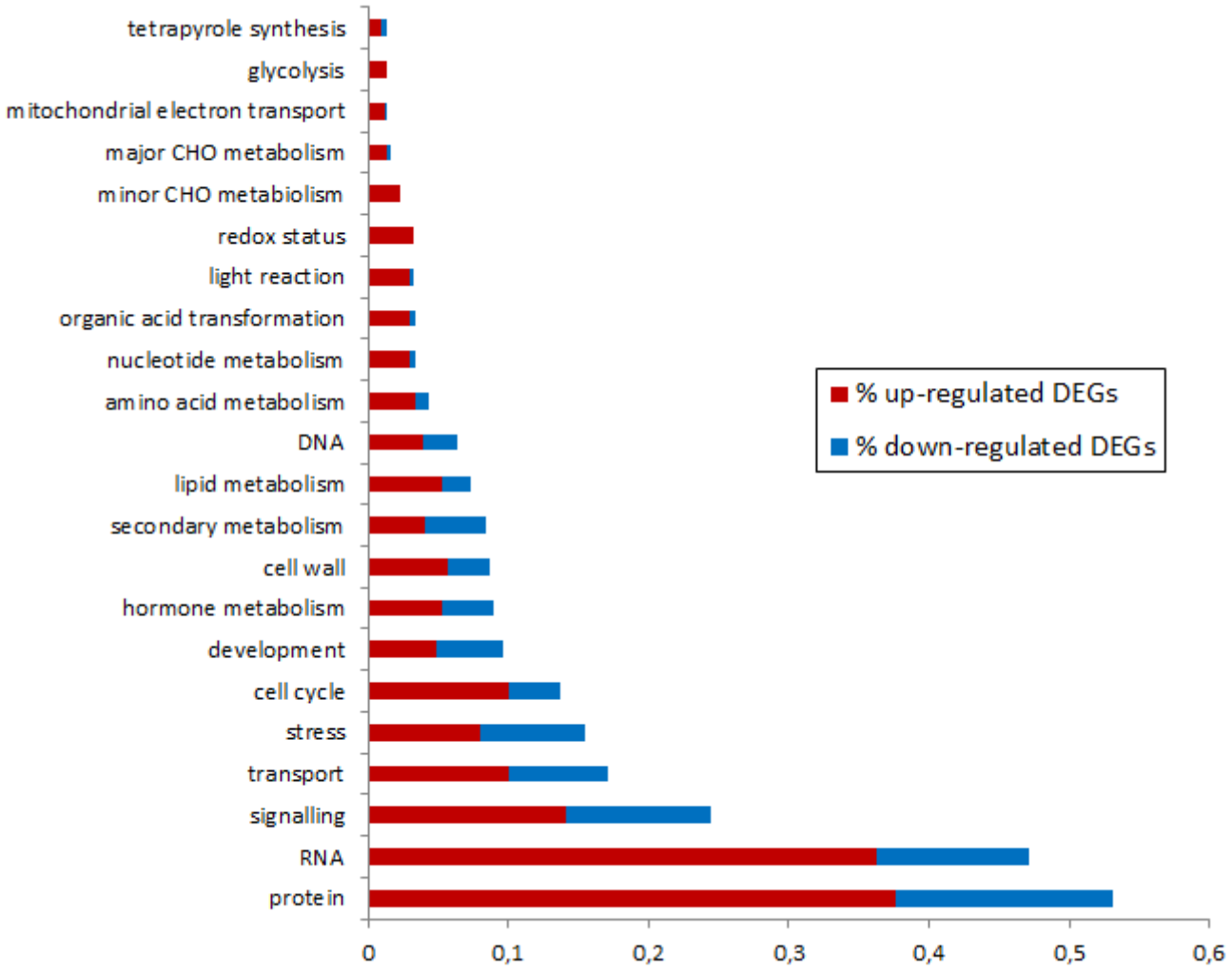
tetrapyrole synthesis
glycolysis
mitochondrial electron transport
major CHO metabolism
minor CHO metabiolism
redox status
light reaction
organic acid transformation
nucleotide metabolism
amino acid metabolism
DNA
lipid metabolism
secondary metabolism
cell wall
hormone metabolism
development
cell cycle
stress
transport
signalling
RNA
protein
0
0,1
0,2
0,3
0,4
0,5
0,6
% up-regulated DEGs
% down-regulated DEGs

Fig. 2

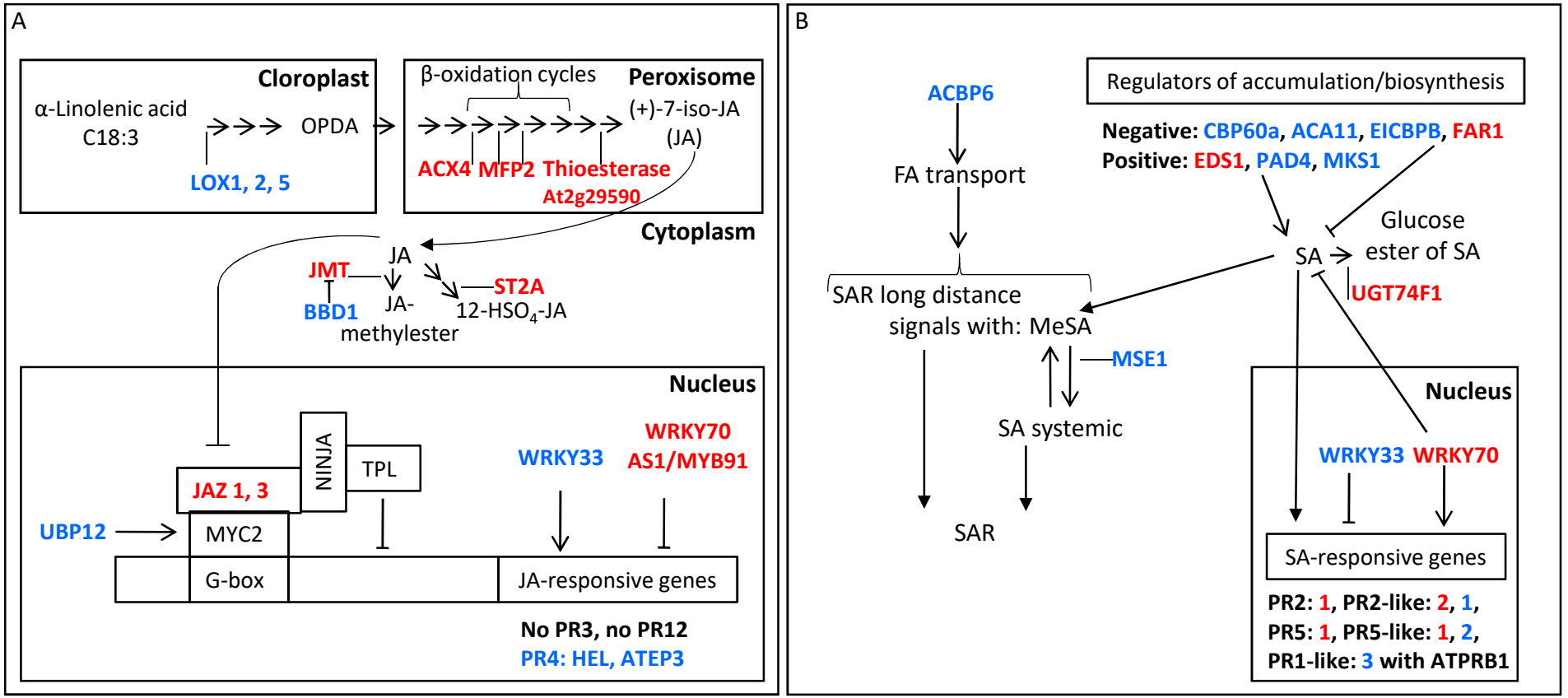
A
Cloroplast
α-Linolenic acid
C18:3
OPDA
LOX1, 2, 5
β-oxidation cycles
Peroxisome
(+)-7-iso-JA
(JA)
ACX4
MFP2
Thioesterase
At2g29590
Cytoplasm
JA
JMT
BBD1
JA-
methylester
ST2A
12-HSO4-JA
Nucleus
NINJA
TPL
JAZ 1, 3
UBP12
MYC2
G-box
WRKY33
WRKY70
AS1/MYB91
JA-responsive genes
No PR3, no PR12
PR4: HEL, ATEP3
B
ACBP6
FA transport
Regulators of accumulation/biosynthesis
Negative: CBP60a, ACA11, EICBPB, FAR1
Positive: EDS1, PAD4, MKS1
SA
Glucose
ester of SA
UGT74F1
SAR long distance
signals with: MeSA
MSE1
SA systemic
SAR
Nucleus
WRKY33
WRKY70
SA-responsive genes
PR2: 1, PR2-like: 2, 1,
PR5: 1, PR5-like: 1, 2,
PR1-like: 3 with ATPRB1

Fig. 3

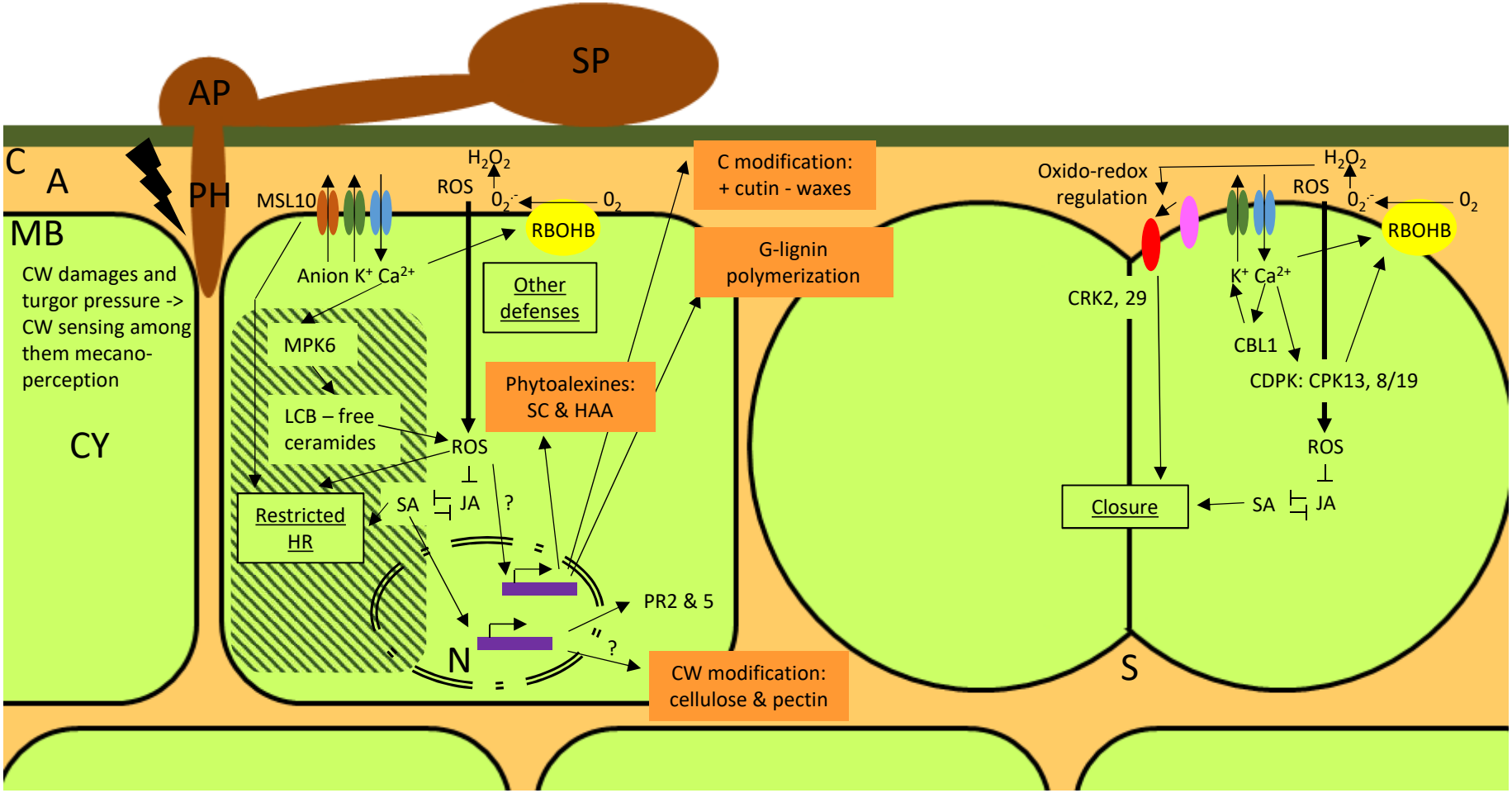
SP
AP
C
A
PH
MB
CW damages and turgor pressure -> CW sensing among them mecano-perception
CY
MSL10
Anion K+ Ca2+
H2O2
ROS
O2.-
O2
RBOHB
Other defenses
C modification: + cutin - waxes
G-lignin polymerization
MPK6
LCB – free ceramides
ROS
Phytoalexines: SC & HAA
Restricted HR
SA
JA
?
PR2 & 5
N
CW modification: cellulose & pectin
Oxido-redox regulation
CRK2, 29
K+ Ca2+
CBL1
CDPK: CPK13, 8/19
Closure
S

Fig. 4

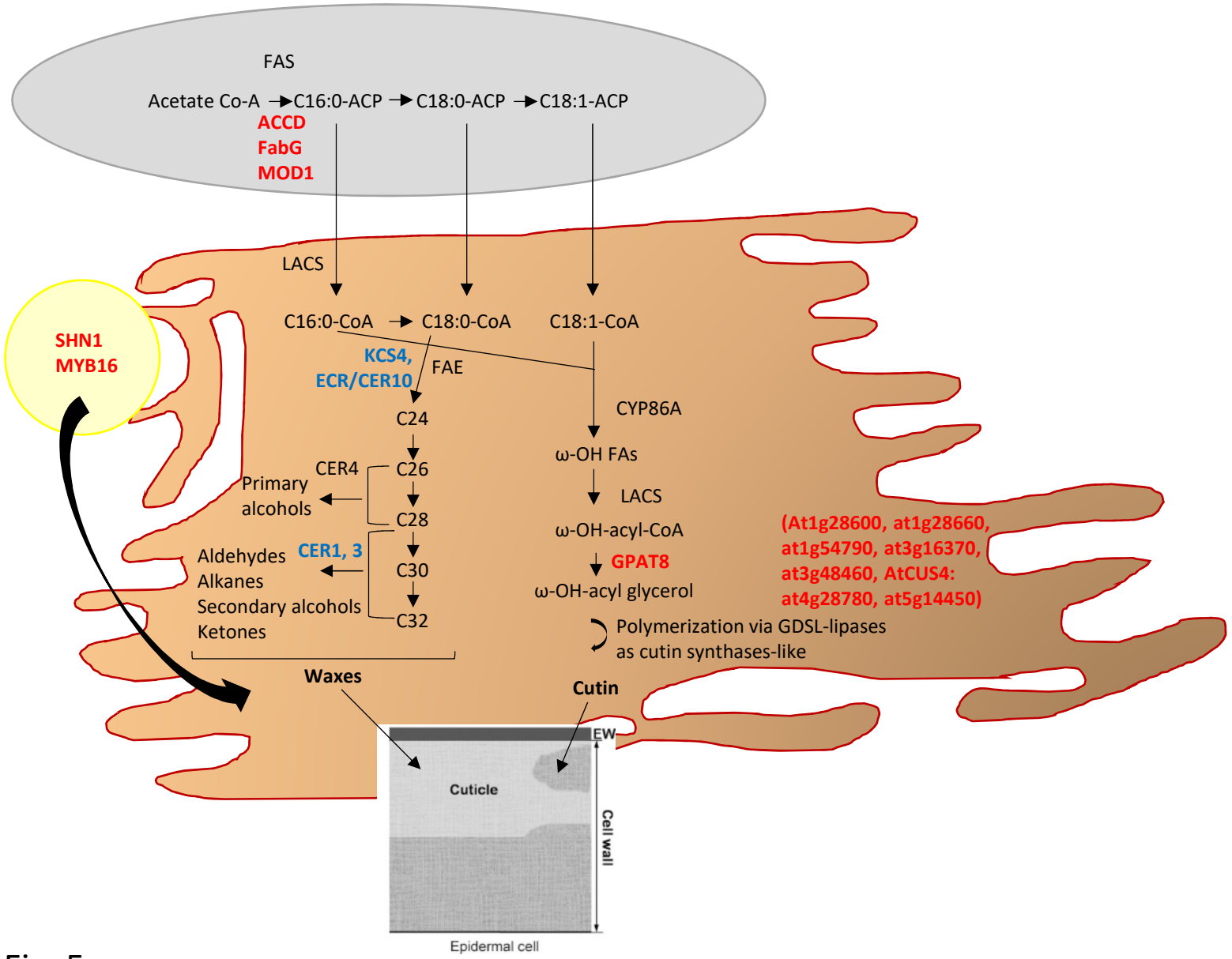
FAS
Acetate Co-A
C16:0-ACP
C18:0-ACP
C18:1-ACP
ACCD
FabG
MOD1
LACS
SHN1
MYB16
C16:0-CoA
C18:0-CoA
C18:1-CoA
KCS4,
ECR/CER10
FAE
CYP86A
C24
ω-OH FAs
CER4
C26
LACS
Primary
alcohols
C28
ω-OH-acyl-CoA
(At1g28600, at1g28660,
at1g54790, at3g16370,
at3g48460, AtCUS4:
at4g28780, at5g14450)
CER1, 3
Aldehydes
Alkanes
Secondary alcohols
Ketones
C30
GPAT8
ω-OH-acyl glycerol
C32
Polymerization via GDSL-lipases
as cutin synthases-like
Waxes
Cutin
EW
Cuticle
Cell wall
Epidermal cell

Fig. 5

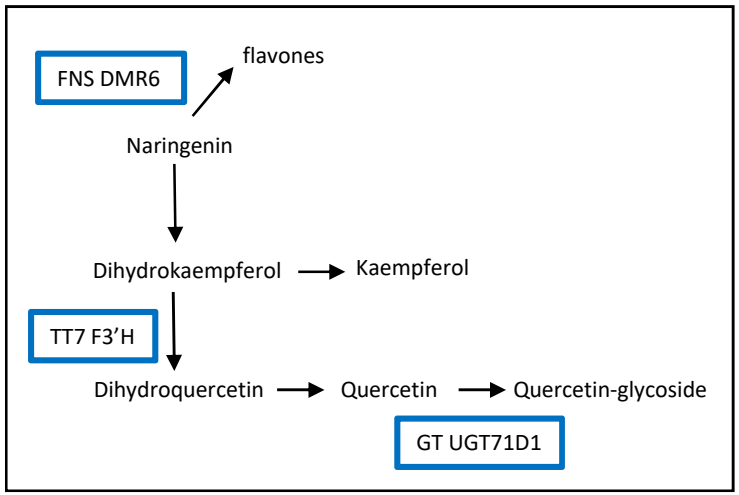
FNS DMR6
flavones
Naringenin
Dihydrokaempferol
Kaempferol
TT7 F3'H
Dihydroquercetin
Quercetin
Quercetin-glycoside
GT UGT71D1

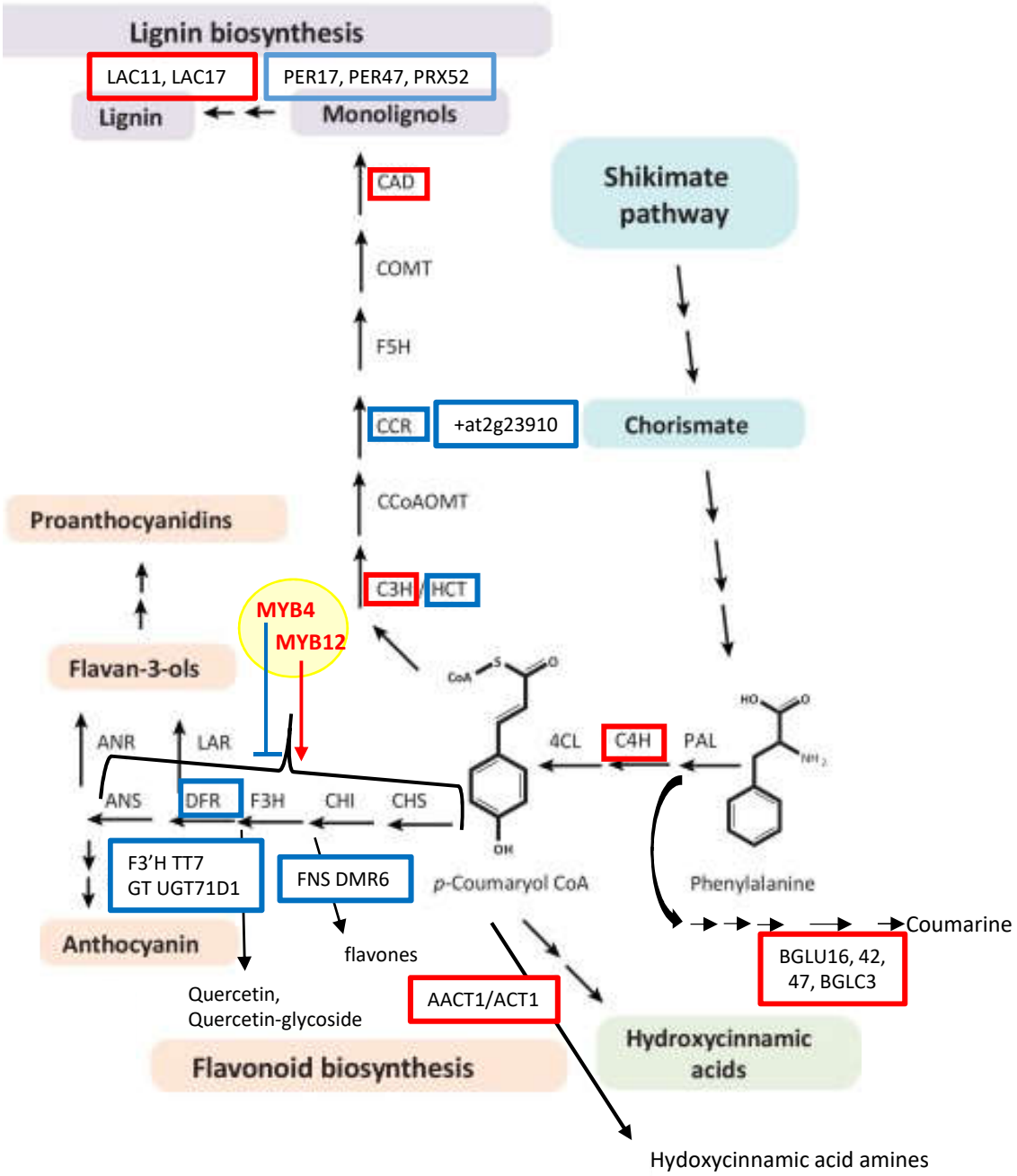
Lignin biosynthesis
LAC11, LAC17
PER17, PER47, PRX52
Lignin
Monolignols
CAD
COMT
F5H
CCR
+at2g23910
CCoAOMT
C3H
HCT
Shikimate pathway
Chorismate
Proanthocyanidins
MYB4
MYB12
Flavan-3-ols
ANR
LAR
ANS
DFR
F3H
CHI
CHS
4CL
C4H
PAL
F3'H TT7
GT UGT71D1
FNS DMR6
p-Coumaryol CoA
Phenylalanine
Coumarine
BGLU16, 42, 47, BGLC3
Anthocyanin
flavones
Quercetin, Quercetin-glycoside
AACT1/ACT1
Hydroxycinnamic acids
Flavonoid biosynthesis
Hydoxycinnamic acid amines

Fig. 6